Aalto-yliopisto
Insinööritieteiden
korkeakoulu

Shanna Myers

Nitrous Oxide and Gas Transfer in Full-Scale Activated Sludge Basins

Master's Thesis submitted for examination for the degree of Master of Science in Technology.

Espoo 25.11.2019
Supervisor: Professor Anna Mikola
Instructors: Dr. Diego Rosso, M. Sc. Kati Blomberg

Aalto University
School of Engineering

Aalto University, P.O. BOX 11000, 00076 AALTO
www.aalto.fi

Abstract of master's thesis

Author Shanna Myers

Title of thesis Nitrous oxide and gas transfer in full-scale activated sludge basins

Master programme Water and Environmental Engineering **Code** ENG29

Thesis supervisor Professor Anna Mikola

Thesis advisors Dr. Diego Rosso, M. Sc. Kati Blomberg

Date 25.11.2019 **Number of pages** 53 + 13 **Language** English

Abstract

Nitrous oxide is a significant greenhouse gas that is a common byproduct of wastewater treatment. Better understanding of nitrous oxide stripping would allow for better models and operational strategies in order to reduce greenhouse gas production from wastewater treatment. To gain insight, simultaneous dissolved and off-gas nitrous oxide and oxygen measurements were taken at the Viikinmäki wastewater treatment plant in Helsinki, Finland during late spring of 2019. During this period, Viikinmäki was experiencing unprecedented high production and emission of nitrous oxide.

In this study, oxygen and nitrous oxide gas transfer kinetics from a full-scale activated sludge basin were compared using a novel measurement setup that shows great potential for further use in gas transfer studies. Oxygen and FTIR analyzers were used simultaneously alongside dissolved gas probes to measure oxygen and nitrous oxide. Oxygen and nitrous oxide relied heavily on aeration to promote mass transfer. However, gas transfer kinetics also depended on dissolved gas concentrations and, in the case of nitrous oxide, production within wastewater. Due to aeration control, oxygen transfer often behaved similarly to steady-state conditions. Nitrous oxide transfer did not reach steady-state conditions in this study to allow for similar mass transfer assumptions.

Three different model approaches were tested to calculate emitted nitrous oxide based on dissolved concentrations. The findings revealed that, while trends in nitrous oxide emission could be reliably modeled, nitrous oxide emissions could not be predicted accurately without a correction factor taking into account changes in wastewater characteristics. Models using a mass transfer coefficient based on diffusivity and experimentally determined oxygen mass transfer coefficients over-estimated nitrous oxide emissions, while a coefficient based on aeration superficial velocity under-estimated off-gas. Therefore, an additional correction factor applied in order to provide good fit between calculated and measured nitrous oxide off-gas varied depending on the model used. Additional variation was caused by wastewater conditions, but no single water quality parameter could be decisively linked to impacts on oxygen or nitrous oxide transfer.

Mass transfer assumptions for this study included constant dissolved gas concentration with depth. In the case of nitrous oxide, this was tested to a depth of 5 meters with a variation of less than 8 %. However, the basins at Viikinmäki are 12 meters deep and additional concentration differences could be undetected at the bottom of the basin. A sensitivity analysis of uncertainties indicated that dissolved nitrous oxide concentrations have a significant impact on calculated off-gas, but the maximum estimated nitrous oxide variation would not substantially undermine calculation accuracy. Further research is recommended to better understand depth profiles in deep basins and water quality conditions that must be accounted for to more accurately model nitrous oxide emissions.

Keywords nitrous oxide, gas transfer, gas stripping, activated sludge, full-scale wastewater treatment plant

Aalto-yliopisto
Insinööritieteiden korkeakoulu

Aalto-yliopisto, PL 11000, 00076 AALTO
www.aalto.fi
Diplomityön tiivistelmä

Tekijä Shanna Myers

Työn nimi Typpioksiduuli ja kaasunsiirto täysimittaisissa aktiivilietealtaissa

Maisteriohjelma Vesi- ja ympäristötekniikka **Koodi** ENG29

Työn valvoja Professori Anna Mikola

Työn ohjaajat FT Diego Rosso, DI Kati Blomberg

Päivämäärä 25.11.2019 **Sivumäärä** 53 + 13 **Kieli** Englanti

Tiivistelmä
Typpioksiduuli on merkittävä kasvihuonekaasu ja tavallinen sivutuote jätevedenpuhdistuksessa. Syvällisempi ymmärrys typpioksiduulin strippaantumisesta mahdollistaisi paremmat mallit ja parannetut toimintastrategiat jätevedenpuhdistamojen kasvihuonekaasupäästöjen vähentämiseksi. Ymmärryksen parantamiseksi liuenneen ja kaasumaisen hapen ja typpioksiduulin määrää mitattiin samanaikaisesti Helsingin Viikinmäen jätevedenpuhdistamolla loppukeväällä 2019. Mittausjakson aikana Viikinmäessä oli ennätyskorkeat typpioksiduulipäästöt.

Tässä tutkimuksessa verrattiin hapen ja typpioksiduulin kaasunsiirtokinetiikoita täysimittaisissa aktiivilietealtaissa käyttämällä uutta tutkimusmenetelmää, jolla osoitettiin olevan suurta potentiaalia myös tulevalle tutkimukselle. Happi- ja FTIR-kaasuanalysaattoreita sekä nestefaasiantureita käytettiin samanaikaisesti hapen ja typpioksiduulin mittaamiseen. Ilmastus vaikutti voimakkaasti hapen ja typpioksiduulin massansiirtoon. Kaasunsiirtokinetiikkaan kuitenkin vaikuttivat lisäksi liuenneiden kaasujen konsentraatiot ja typpioksiduulin tapauksessa myös sen tuotanto jätevedessä. Ilmastusohjauksen takia hapen siirto käyttäytyi usein samalla tavoin kuin tasapainotilassa. Typpioksiduulin siirto ei saavuttanut tasapainotilaa tässä tutkimuksessa eikä siten mahdollistanut samanlaisia massansiirto-oletuksia.

Kolmea erilaista mallinnuksen lähestymistapaa testattiin laskettaessa typpioksiduulipäästöjä liuenneiden pitoisuuksien perusteella. Tulokset paljastivat, että vaikka typpioksiduulipäästöjen kehityssuuntauksia voitiin luotettavasti mallintaa, typpioksiduulipäästöjä ei voitu ennustaa tarkasti ilman korjauskerrointa, joka ottaa huomioon jäteveden ominaisuuksien muutokset. Mallit, joissa käytetään diffusiivisuuteen perustuvaa massansiirtokerrointa ja kokeellisesti määritettyä hapen massansiirtokerrointa, yliarvioivat typpioksiduulinpoistoa. Toisaalta kerroin, joka perustuu ilmastuksen pintanopeuteen, aliarvioi siirtoa. Siksi lasketun ja mitatun typpioksiduulin poistokaasun hyvän yhteensopivuuden aikaansaamiseksi käytetty lisäkorjauskerroin vaihteli käytetyn mallin mukaan. Lisävaihteluita aiheuttivat jäteveden ominaisuudet, mutta yhtäkään vedenlaatuparametria ei voitu liittää ratkaisevasti hapen tai typpioksiduulin siirron vaikutuksiin.

Tämän tutkimuksen massansiirto-oletuksiin sisältyi liuenneen kaasun konsentraation vakio tietyllä syvyydellä. Typpioksiduulin tapauksessa vakiota testattiin 5 metrin syvyyteen saakka. Vaihtelu oli alle 8 %. Viikinmäen altaat ovat kuitenkin 12 metriä syviä ja mahdollisia lisäeroja voitaisiin havaita altaan pohjassa. Epävarmuustekijöiden herkkyysanalyysi osoitti, että liuenneilla typpioksiduulipitoisuuksilla on merkittävä vaikutus laskettuun poistokaasuun, mutta suurin arvioitu typpioksiduulin pitoisuudenmuutos ei heikennä olennaisesti laskentatarkkuutta. Jatkotutkimuksia suositellaan syvien altaiden syvyysprofiilien ja veden laatuolosuhteiden ymmärtämiseksi paremmin, jotta typpioksiduulipäästöjen voidaan mallintaa tarkemmin.

Avainsanat typpioksiduuli, kaasunsiirto, kaasustrippaus, aktiiviliete, täyden mittakaavan jätevedenpuhdistamo

Preface

The research for this master's thesis was conducted at the Viikinmäki wastewater treatment plant in Helsinki, Finland as part of a long-term study on reducing and mitigating nitrous oxide emissions from wastewater treatment. This research was financially supported by Helsinki Region Environmental Services Authority (HSY), Aalto University, and the Finnish Water Utilities Association (FIWA) development fund.

I would like to thank my thesis advisory committee: professors Anna Mikola and Diego Rosso and M. Sc. Kati Blomberg. Thanks for all your help with background research, thesis review and comments, and for your patience and encouragement. Anna, it was a pleasure to work for you while at Aalto and many thanks for your guidance on this thesis. Diego, thanks for coming to the treatment plant with me and getting your gloves dirty. Kati, thanks for all the times you redirected me and helped me to narrow down my scope.

Thanks to the HSY staff at Viikinmäki, especially Anna Kuokkanen for all the assistance and the data sets you have sent my way. Thank you to Kari Murtonen and Marko Elo for on-site assistance. Thanks also to rest of the staff for allowing me to join coffee breaks and attempt to solve Finnish quizzes with you. Special thanks to fellow Aalto students Heini Snellman and Suvi Ojala for their assistance with on-site research, Kiia Molsä and Henna Jylhä for translation help, Maija Vilpanen for pH and depth analysis data, and to everyone who helped in any way with my thesis work.

Additional thanks to the laboratory team from the water building; Antti Luohio, Aino Peltola, and Marina Sushko; for construction and technological assistance, laboratory assistance, and for lending me probes and lab space. To the WAT crew as a whole: it has been a pleasure to learn and work alongside all of you these past 2 years. Finally, to all the friends and family who have helped along the way: thank you for encouraging me, laughing with me, and for putting up with me talking about wastewater all the time.

"Now to Him who is able to do immeasurably more than all we ask or imagine, according to his power that is at work within us, to Him be glory in the church and in Christ Jesus throughout all generations, for ever and ever! Amen." (Ephesians 3:20-21)

Espoo 25.11.2019

Shanna G Myers

Shanna Myers

Table of Contents

List of Figures

List of Tables

Abbreviations

Acronyms and Initialisms

AE	Aeration efficiency
ASM3	Activated sludge model number 3
COD	Chemical oxygen demand
COD/N	Ratio of chemical oxygen demand to nitrogen
DO	Dissolved oxygen
EF	Emission factor
EU	European Union
FIWA	Finnish Water Utilities Association
FTIR	Fourier transform infrared
GWP-100	100-year global warming potential
HSY	Helsingin Seudun Ympäristöpalvelut/ Helsinki Region Environmental Services Authority
IPCC	Intergovernmental Panel on Climate Change
OTE	Oxygen transfer efficiency
OTR	Oxygen transfer rate
OUR	Oxygen uptake rate
RAS	Return activated sludge
SOTE	Standard oxygen transfer efficiency
SRT	Sludge retention time
SS	Suspended solids
SSE	Sum of squared errors
TN	Total nitrogen
U.S.	United States (of America)
WWTP	Wastewater treatment plant

Chemicals

Symbol	Chemical Name	Chemical Name (Finnish)
CH_3OH	Methanol	Metanoli
CH_4	Methane	Metaani
CO	Carbon monoxide	Hiilimonoksidi
CO_2	Carbon dioxide	Hiilidioksidi
$Ca(OH)_2$	Calcium hydroxide, Lime	Kalsiumhydroksidi, Sammutettu kalkki
$FeSO_4$	Ferric sulphate	Ferrosulfaatti
NH_2OH	Hydroxylamine	Hydroksyyliamiini
NH_3	Ammonia	Ammoniakki
NH_4^+	Ammonium	Ammoniumioni
N_2	Nitrogen	Typpi
NO	Nitric oxide	Typpioksidi
N_2O	Nitrous oxide	Typpioksiduuli
NO_2^-	Nitrite	Nitriitti
NO_3^-	Nitrate	Nitraatti
NaOH	Sodium hydroxide	Natriumhydroksidi
O_2	Oxygen	Happi

Symbols

A	[m^2]	Area
A_B	[m^2]	Surface area of single bubble
A_G	[m^2]	Surface area of gas-liquid interface (surface area of all bubbles)
AE	[kg O_2/kWh]	Aeration efficiency
C	[mg/L]	Concentration
C_G	[mg/L]	Gaseous concentration
C_L	[mg/L]	Dissolved gas concentration
C_s	[mg/L]	Saturation concentration (in liquid)
C^*	[mg/L]	Equilibrium concentration at gas-liquid interface
d_L	[m]	Reference depth of aeration array in lab setup
d_R	[m]	Depth of aeration array in full-scale reactor
D_{N2O}, D_{O2}	[m^2/d]	Diffusivity coefficients of N_2O, O_2
EF	[%]	Emission factor
H	[-]	Unitless Henry's coefficient
$H_{p/x}$	[bar]	Henry's coefficient (partial pressure per molar ratio)
F	[-]	Aeration membrane fouling factor
j	[-]	Number of blank values preceding x_n
k	[-]	Number of blank values following x_n
K_L	[m/d]	Liquid-side mass-transfer coefficient
K_La	[1/d]	Liquid-phase volumetric mass transfer coefficient
MW	[kg/mol]	Molar mass
n_b	[-]	number of bubbles within tank
OTE	[%]	Oxygen transfer efficiency
OTR	[kg O_2/h]	Oxygen transfer rate
OUR	[kg/m^3/h]	Oxygen uptake rate
P	[kW]	Power use of aeration
Q_A	[m^3/d]	Air flowrate
Q_{WW}	[m^3/d]	Wastewater flowrate
R	$\left[\frac{L*bar}{mol*K}\right]$	Ideal gas constant
r	[mg/L/d]	Uptake rate
SOTR	[kg O_2/h]	Standard oxygen transfer rate
t	[d]	Time
T	[K]	Temperature
T_C	[°C]	Temperature in Celsius
v_g	[m^3/m^2/s]	Superficial velocity
V	[m^3]	Volume
V_B	[m^3]	Volume of single bubble
V_G	[m^3]	Volume of gas (sum of all gas bubbles)
V_L	[m^3]	Liquid volume
x_n	[-]	Blank value to fill for data extrapolation
α	[-]	Wastewater gas transfer correction factor
β	[-]	Wastewater solubility correction factor
θ	[-]	Temperature conversion factor
ρ	[kg/L]	Density
$\frac{\Delta H_{sol}}{R}$	[K]	Temperature dependence term

Equations

$$\frac{\partial C}{\partial t} = K_L a * (C_L - C^*) - r \quad (1)$$

$$K_L a_{N_2O} = K_L a_{O_2} * \sqrt{\frac{D_{N_2O}}{D_{O_2}}} \quad (2)$$

$$\frac{\partial C}{\partial t} = \alpha * K_L a * (C_L - \beta C^*) - r \quad (3)$$

$$V_B \frac{dC_G}{dt} = K_L * A_B * \left(C_L - \frac{C_G}{H}\right) \quad (4)$$

$$\frac{A_B}{V_B} = \frac{aV_L}{V_G} \quad (5)$$

$$\frac{\partial C_G}{\partial t} = (\alpha) * K_L a * \frac{V_L}{V_G} * (C_L - \frac{C_G}{H}) \quad (6)$$

$$C_{G,out} = C_{G,in} * e^{-\frac{(\alpha)*K_L a*\frac{V_L}{V_G}*t}{H}} + H * C_L * \left(1 - e^{-\frac{(\alpha)*K_L a*\frac{V_L}{V_G}*t}{H}}\right) \quad (7)$$

$$C_{G,out} = C_{G,in} * e^{-\frac{(\alpha)*K_L a*V_L}{H*Q_A}} + H * C_L * \left(1 - e^{-\frac{(\alpha)*K_L a*V_L}{H*Q_A}}\right) \quad (8)$$

$$H_{p/x} = H_{p/x\_0} * e^{\frac{\Delta H_{sol}}{R}\left(\frac{1}{T}-\frac{1}{T_0}\right)} \quad (9)$$

$$H = H_{p/x} * \frac{MW_{H_2O}}{\rho_{H_2O}} * \frac{1}{RT} \quad (10)$$

$$H = \left(H_{p/x\_0} * e^{\frac{\Delta H_{sol}}{R}\left(\frac{1}{T}-\frac{1}{T_0}\right)}\right) * \frac{MW_{H_2O}}{\rho_{H_2O}} * \frac{1}{RT} \quad (11)$$

$$K_L a_T = K_L a_{T=20C} * \theta^{(T_C-20)} \quad (12)$$

$$K_L a = \frac{Q_A * C_G}{V_L * (C_S - C_L)} \quad (13)$$

$$K_L a_F^* = \left(\frac{d_R}{d_L}\right)^{-0.49} * \left(34500 * v_g\right)^{0.86} \quad (14)$$

$$OTR = SOTR * \alpha * F * \left(\frac{\beta C_{\bar{S},T,H} - C_L}{C_{s,20}}\right) * 1.024^{(T_C-20)} \quad (15)$$

$$OTR = \frac{1}{24} K_L a * (C_s - C_L) * V * 10^{-3} \quad (16)$$

$$OUR = \frac{OTR}{V} \quad (17)$$

$$AE = \frac{OTR}{P} \quad (18)$$

$$OTE = \frac{OTR}{W_{O_2}} \sim \frac{O_{2,in} - O_{2,out}}{O_{2,in}} \quad (19)$$

$$EF = \frac{C_{N_2O-N,eff} * Q_{A,eff}}{C_{TN,inf} * Q_{WW,eff}} \quad (20)$$

$$x_n = \frac{\sum_{i=j+1}^{k+1}[x_{n-i}] + \sum_{i=k+1}^{j+1}[x_{n+i}]}{j+k+2} \quad (21)$$

1 Introduction

Nitrous oxide (N_2O) is a potent greenhouse gas and ozone-depleting chemical with a 100-year global warming potential approximately 300 times greater than carbon dioxide (IPCC, 2013). Globally, most N_2O (61 %) is emitted from natural sources such as microbial activity in soils and the ocean (IPCC, 2013). However, N_2O is also released from anthropogenic sources. It is estimated that agriculture, fuel combustion, and wastewater treatment account for 74 %, 8 %, and 1.4 % of anthropogenic N_2O in the U.S., respectively, and 67 %, 20 %, and 3 % of global anthropogenic N_2O, respectively (EPA, 2019; IPCC, 2013).

Wastewater treatment has traditionally focused on reducing pollutant and excess nutrient discharge to waterways, but in recent years there has been increased regulatory interest in air emissions, especially greenhouse gas emissions, from wastewater treatment (EPA, 2016; EU Parliament, 2006; IPCC, 2006). Methods for estimating N_2O emissions have been recommended, including the updated Intergovernmental Panel on Climate Change (IPCC) single emission factor (EF) that proposes a percent emission based off the type of wastewater treatment and influent nitrogen load (IPCC, 2019). However, a review of recent N_2O studies from wastewater treatment plants all over the world revealed significant variability between N_2O generation per influent nitrogen load (Vasilaki, et al., 2019).

There is a desire for increased accuracy in estimating N_2O emissions from individual treatment plants in order to further develop operational strategies to reduce greenhouse gas emissions. Dissolved N_2O concentrations can be used to estimate N_2O emissions using gas transfer equations (Baresel, et al., 2016), and attempts have been made to determine the approximate gas transfer coefficients for N_2O in clean water and wastewater (Foley, et al., 2010; Mampaey, et al., 2015). However, gas transfer coefficients are specific to wastewater conditions and wastewater conditions vary with time and location. There is currently very limited published work comparing continuous measurements of dissolved and off-gas N_2O concentrations from the same time and place.

Mass transfer kinetics for N_2O are often estimated using O_2 mass transfer kinetics, and some studies assume the impact of wastewater conditions on oxygen (O_2) and N_2O transfer to be analogous (Fiat, 2019; Foley, et al., 2010; von Schulthess, et al., 1995). However, the relationship between changes in wastewater quality and changes in N_2O transfer is relatively unknown compared to O_2 transfer. No method exists yet for measuring O_2 transfer from the same location as N_2O flux. Similarly, there is no prior research on N_2O stripping alongside O_2 transfer.

The Viikinmäki wastewater treatment plant (WWTP) in Helsinki, Finland is remarkably suitable for measuring greenhouse gas generation due to the entire plant being enclosed underground. The Helsinki Region Environmental Services Authority (HSY) began studies on N_2O and other gas emissions from Viikinmäki in 2007, and continuous online monitoring of air emissions began in 2012 (Kosonen, 2013). Continuous online monitoring of dissolved

N_2O began in 2016 in two activated sludge basins (Blomberg, 2016). The activated sludge basins at Viikinmäki are 12 meters deep, much deeper than at most treatment plants, so possible changes with depth should be more significant than in shallow basins.

This thesis aims to reduce the knowledge gap on localized N_2O stripping and compare the variation in N_2O stripping kinetics to the variation in O_2 transfer kinetics. The primary objectives of this thesis were to study the production and off-gas of N_2O in the activated sludge basins at Viikinmäki and to compare N_2O and O_2 transfer. To accomplish this, a method for simultaneous measurement of N_2O and O_2 was developed. Additional objectives included supporting efforts to model and estimate N_2O production at Viikinmäki, assessing depth variability of N_2O at Viikinmäki to support simplifying gas transfer assumptions, and comparing calculated gas transfer coefficients from this study against published values.

In order to gain insight on N_2O stripping, a novel method for simultaneous N_2O and O_2 measurement was tested. An O_2 analyzer and a continuous gas measurement FTIR device were connected to a modular off-gas hood while hand probes and Viikinmäki's dissolved N_2O probes were used near the floating hood in order to record dissolved and emitted N_2O and O_2 at the same time and location. The purpose of this simultaneous measurement was to provide a comparison between O_2 and N_2O behavior in the activated sludge basins as well as information on O_2 transfer efficiency. Improved understanding of stripping, paired with reliable N_2O production models, would allow WWTPs to realistically model N_2O production under different operational strategies in order to optimize wastewater treatment for maximum nutrient removal and minimum greenhouse gas emissions.

This thesis is part of ongoing N_2O research within the Water and Environmental Engineering department at Aalto University. Previous studies have included N_2O production in Finnish wastewater plants with different process configurations (Leppänen, 2012), long-term monitoring of N_2O emissions from Viikinmäki (Kosonen, 2013), and modeling N_2O production at Viikinmäki using an ASM3 model (Blomberg, 2016). This work was limited to considering the gas transfer behavior during the measurement campaign and does not consider the effects of seasonal or yearly variability of N_2O emissions. Additionally, the biological reactions and chemical interactions influencing N_2O production are only briefly considered.

2 Nitrous Oxide and Gas Transfer

2.1 Nitrous Oxide in Wastewater Treatment

2.1.1 Production and Emission of Nitrous Oxide

Nitrous oxide, commonly known as laughing gas, is a greenhouse gas that, as of 2009, is also the top ozone-depleting emission (NOAA, 2009). The average measured atmospheric N_2O concentration was 330 ppb in 2017 (NOAA, 2019). Agriculture is the key contributor to anthropogenic N_2O emissions, but other significant sources include transportation, fuel combustion, industrial sources, and waste management. Waste management includes wastewater treatment, which contributes 1.4-3 % of the global N_2O load (EPA, 2019; IPCC, 2013). The greenhouse impact of gases is commonly measured using the 100-year global warming potential (GWP-100), defined as the ratio of the cumulative radiative forcing induced over 100 years by 1 kg of that gas compared to 1 kg of carbon dioxide (CO_2). The GWP-100 can be calculated with or without climate-carbon feedback, the estimated impact on the earth's carbon cycle caused by the increased radiative forcing of a gas (Gasser, et al., 2017). The GWP-100 of N_2O is calculated as 265 without climate-carbon feedback and 298 with feedback (IPCC, 2013).

Based on current knowledge, N_2O in wastewater is considered to be produced primarily through biological pathways during nitrification and denitrification of wastewater. In nitrification, ammonia and ammonium (NH_3 and NH_4^+) are oxidized by nitrifying bacteria into nitrite (NO_2^-) and then nitrate (NO_3^-). Denitrification is the process by which denitrifying bacteria reduce NO_3^- back to NO_2^- and then to nitrogen gas (N_2), with nitric oxide (NO) and N_2O as intermediaries between NO_2^- and N_2. The three major biological pathways recognized to produce N_2O are nitrifier denitrification, hydroxylamine oxidation, and incomplete heterotrophic denitrification (Hanaki, et al., 1992; Wunderlin, et al., 2012; Zheng, et al., 1994). Denitrification reactions produce and consume N_2O, and denitrification is the only known N_2O sink within wastewater treatment plants (Thomson, et al., 2012). The production and consumption pathways for N_2O are illustrated in Figure 1 on the following page. Chemical pathways to N_2O production also exist, but these are often influenced by bacterial activity (Kampschreur, et al., 2009).

Figure 1. Three main microbial N_2O production pathways (Duan, et al., 2017). Abbreviations: AOB – ammonia oxidizing bacteria; AMO – ammonium monooxygenase; HAO – hydroxylamine oxidoreductase; NirK – copper-containing nitrite reductase; NorB – membrane-bound nitric oxide reductase; NaR – nitrate reductase; NiR – nitrite reductase; NOR – nitric oxide reductase; N_2OR – nitrous oxide reductase. *Unidentified NiR alternate to NirK active in AOB (Kozlowski, et al., 2014).

Understanding the conditions that influence N_2O production is key to optimizing wastewater treatment for lower greenhouse gas emissions. Low dissolved oxygen (DO) during nitrification or aerobic conditions during denitrification leads to increased N_2O emissions (e.g. Kampschreur, et al., 2009; Tallec, et al., 2006), as does increased NO_2^- accumulation in both nitrification and denitrification (Hanaki, et al., 1992; Kampschreur, et al., 2007). Vasilaki et al. (2018) found changes in N_2O concentrations were often linked to changes in process concentrations of NH_4^+, NO_2^-, and NO_3^- or to changes in influent flowrate and temperature. Parameters affecting emissions as identified by Kampschreur et al. (2009) are shown in Figure 2.

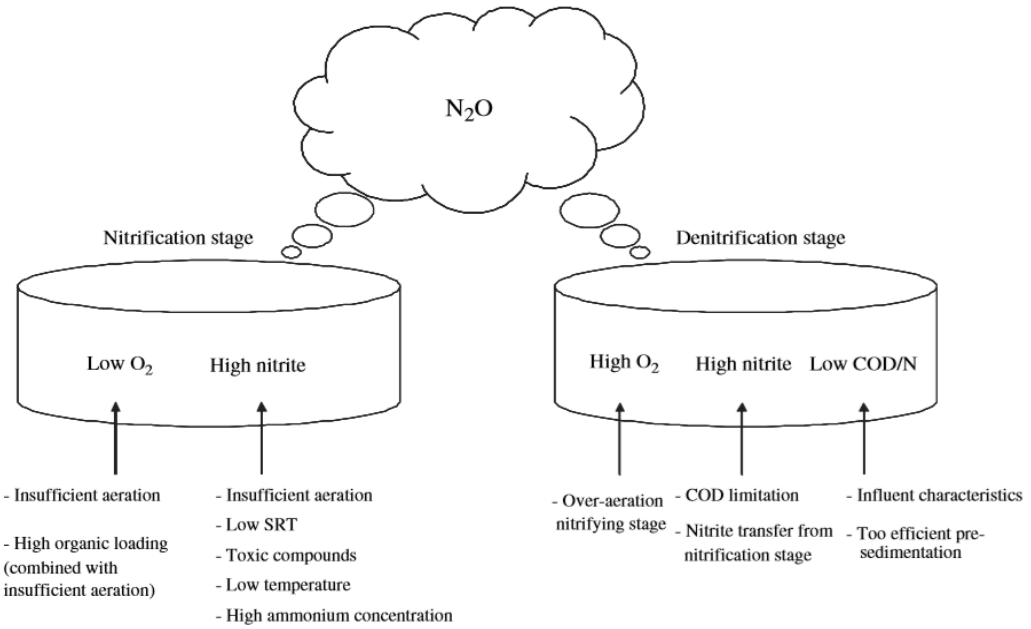

Figure 2. Identified key parameters resulting in N_2O emissions (Kampschreur, et al., 2009). Abbreviations: SRT – sludge retention time, COD – chemical oxygen demand, COD/N – ratio of COD to nitrogen.

2.1.2 Quantifying Emissions

In order to determine N_2O emissions from WWTPs, there must be a way to reliably measure or estimate production and off-gas. In many prior studies, either dissolved or gaseous N_2O were measured. Gaseous N_2O can be measured accurately with gas chromatograph analysis of grab samples from treatment basin off-gas (e.g. Czepiel, et al., 1995; Hanaki, et al., 1992; Pascale, et al., 2017; von Schulthess, et al., 1995) or, more recently, off-gas N_2O can be measured using infrared analyzers (e.g. Ahn, et al., 2010a; Bellandi, et al., 2018; Tallec, et al., 2006; Wunderlin, et al., 2012). Dissolved N_2O concentrations can be determined through extraction into headspace followed by gas chromatograph analysis (e.g. Hall, 1980; Kosse, et al., 2017; Townsend-Small, et al., 2011) or using probes (e.g. Ahn, et al., 2010a; Baresel, et al., 2016; Foley, et al., 2010; Kampschreur, et al., 2008).

Dissolved N_2O probes have received mixed reviews for their utility in the past decade. In a 2010 study, Yu et al. found microelectrode dissolved N_2O probes (Unisense, Denmark) to experience significant interference from dissolved NO and O_2. As a result, one author of this study suggested that, although good correlation was seen between measured gaseous and dissolved N_2O, dissolved N_2O concentrations should be "alternately approximated based on estimated system-specific gas-liquid mass transfer coefficients" (Chandran, 2011). Other studies had greater success measuring with dissolved N_2O probes. Ahn et al. (2010a) found measured dissolved N_2O from a Clark-type polarographic N_2O sensor (Unisense, Denmark) roughly followed the same trends as continuous gaseous N_2O measurements using an infrared gas filter correlation (Teledyne API, California) in a data set with limited overlapping measurements. Kampschreur et al. (2008) used a modified Clark electrode N_2O probe (Unisense, Denmark) to measure dissolved N_2O alongside gas chromatograph analysis of gas samples. They also saw a similar trend between dissolved and gaseous N_2O, and a 10-fold decrease in dissolved N_2O was recorded simultaneously with a 10-fold decrease in gaseous N_2O. Additional studies in the past decade using dissolved N_2O probes suggest that the accuracy of these probes is sufficient to provide useful data (e.g. Baresel, et al., 2016; Blomberg, 2016; Foley, et al., 2010).

The relationship between emitted and dissolved N_2O concentrations (and vice versa) is well established via gas transfer equations (covered further in section 2.2) and there are studies in which liquid concentrations of N_2O are calculated using off-gas N_2O concentrations, maximum N_2O solubility, and estimated or calculated mass transfer values (e.g. von Schulthess, et al., 1995; Yu, et al., 2010). However, these estimations still require measuring either gaseous or dissolved N_2O. To simplify calculations for WWTPs without N_2O measurements, the IPCC developed guidelines for calculating emissions using an average emission factor (EF). This EF is defined as the N_2O emitted (in kg-N) per kg of total nitrogen (TN) contained in wastewater, though it can also be expressed as a percentage. In IPCC calculations, the EF is based on influent TN, a method that does not consider the efficiency or percent nitrification in WWTPs. To account for emissions caused by untreated nitrogen load, the IPCC has a separate EF for TN released to the environment (IPCC, 2019).

2.1.3 Variations in Nitrous Oxide Production

In their 2006 guidelines, the IPCC estimated an N_2O production of 3.2 g/person/year in WWTPs with biological nitrogen removal (IPCC, 2006). This value was based off the first N_2O study in the US by Czepiel et al. (1995) at a WWTP receiving only municipal wastewater. Studies on N_2O production at other WWTPs found many different values for N_2O production, suggesting this first value was not fully representative. The 2006 guidelines have since been refined to better reflect the variations between emissions at different WWTPs, and EFs are now based on treated nitrogen load instead of population. For their 2019 refinement, the IPCC performed a literature review and found the average municipal WWTP with centralized aerobic treatment had an EF of 1.6 % of influent TN as N_2O. However, this EF was found to vary from 0.016 to 4.5 % between studies performed at different WWTPs (IPCC, 2019). Another review of N_2O emissions monitoring studies from the past decade by Vasilaki et al. (2019) found N_2O EFs of 0.03 to 5.6 % of influent TN.

There is clearly significant variation in the percent of influent nitrogen that is released to the atmosphere as N_2O from different WWTPs. Much of this variation is attributed to differences in the process conditions that were mentioned in section 2.1.1. However, within a single WWTP there are daily and seasonal variations in wastewater conditions leading to variations in emitted N_2O concentrations (e.g. Daelman, et al., 2015; Emami, et al. 2018; Kampschreur, et al., 2008; Kosonen, et al., 2016).

There is also variation in N_2O production from different processes in the same WWTP. Studies at various plants have typically found that N_2O is released from processes where gas stripping occurs, primarily from aeration basins (e.g. Ahn, et al., 2010b; Law, et al., 2012). However, Foley et al. (2010) have reported N_2O production via denitrification during secondary settling and Mikola et al. (2014) recorded significant emissions of N_2O from the secondary settling basins at Viikinmäki. Caivano et al. (2017) also measured N_2O from a turbulent post-chlorination well, with N_2O production occurring due to the reaction of hydroxylamine (NH_2OH) with chlorine. Since N_2O emission is affected both by N_2O production and by gas stripping, local variations in aeration and microbial activity within a single aeration basin would result in local variations in N_2O emissions. These local variations can result from fouling, unequal mixing, changes in water quality, damaged aeration equipment, and other process inconsistencies (Rosso, 2018). Due to these many sources of variability, estimations of yearly N_2O emissions should be based off measurements that representatively include temporal and spatial variation in N_2O emissions.

2.2 Gas Transfer in Aeration Basins

2.2.1 Gas Transfer Equations

Mass transfer across a liquid-gas interface is based on two-film theory, in which molecular diffusion between liquid and gas is modeled as occurring between two stagnant films (Lewis & Whitman, 1924). Flux of a substance across the gas and liquid films are governed by gas and liquid transfer coefficients as well as the respective gas and liquid concentrations of that substance. In the case of liquid-phase limited transfer for sparingly soluble gases, this liquid-side coefficient dominates and mass transfer can be modeled with the following equation (Lewis & Whitman, 1924):

$$\frac{\partial C}{\partial t} = K_L a * (C_L - C^*) - r \quad [1]$$

Where:

K_La = liquid-side mass transfer coefficient, including the ratio of surface area of liquid-gas interface to liquid volume [d^{-1}];
r = uptake rate, negative if the substance is produced instead of consumed [mg/L/d];
C_L = dissolved gas concentration in the bulk liquid [mg/L]; and
C^* = dissolved gas concentration at the liquid-gas boundary, which is assumed to be in equilibrium with the gas concentration [mg/L].
Liquid-gas equilibrium is determined by the unitless Henry's coefficient (H) and the gas concentration (C_G): $C^* = \frac{C_G}{H}$

Volumetric mass transfer coefficients can be determined experimentally through many methods. Most commonly, WWTPs are interested in solving for the K_La for O_2 due to the important role of O_2 in biological treatment of wastewater and the associated energy costs of aeration (WEF, 2009). In the American Society of Civil Engineers standard method for measuring O_2 transfer in clean water, sodium sulfite with cobalt chloride as a catalyst is used to fully remove DO and the water is then re-aerated to near saturation while using DO probes to track the DO and calculate K_La (ASCE, 2007). Another commonly used method for K_La determination that works in wastewater with established aerobic bacteria is the dynamic method (Bandyopadhyay & Humphrey, 1967), which requires stopping and re-starting aeration and measuring the resulting changes in DO. To accurately determine K_La values with either method, DO electrodes with fast response times are necessary (Moutafchieva, et al., 2013).

Volumetric mass transfer coefficients are gas-specific, but the same methods for O_2 K_La determination cannot be easily applied to all gases. By applying the penetration theory (Higbie, 1935) it is possible to estimate K_La using a known K_La value for a separate gas and the respective diffusion coefficients for both gases, as has been done in other studies (e.g. Fiat, 2019; Lizarralde, et al., 2018). This only applies in cases where both gases have similar, low solubilities and diffusion coefficients must be measured under the same conditions.

To theoretically solve for N_2O using O_2 values, the equation would be as follows:

$$K_L a_{N_2O} = K_L a_{O_2} * \sqrt{\frac{D_{N_2O}}{D_{O_2}}} \quad [2]$$

Where:
D_{N_2O} = diffusion coefficient of N_2O in water [m^2/d], and
D_{O_2} = diffusion coefficient of O_2 in water [m^2/d].

Mass transfer will occur at different rates in clean water than in wastewater, as K_La is also liquid-specific. For wastewater applications, equation 1 is often modified to the following form to account for the difference between clean water and wastewater:

$$\frac{\partial C}{\partial t} = \alpha * K_L a * (C_L - \beta C^*) - r \quad [3]$$

Where:
α = correction factor for gas transfer rate in wastewater compared to clean water, and
β = correction factor for maximum solubility in wastewater, usually based off salinity.

For mass transfer through bubbles in aeration the K_La, which includes the ratio of surface area to volume, is constantly changing due to the dynamic nature of bubble surface area (De Temmerman, et al., 2015). In practice, the K_La used for calculations is often an average value based on a limited range of conditions. As a result, the alpha correction factor frequently includes the effects of bubble geometry in addition to the effects of wastewater composition. When using a static K_La value, it is more accurate to represent the dynamic nature of gas transfer using a dynamic alpha (Jiang, et al., 2017; Rosso, 2018). However, the use of static alpha factors is more common due to the increased complexity and computational resources necessary to calculate the alpha factor dynamically.

Equation 3 can be modified and used for any sparingly soluble gas, but the impact of water quality on mass transfer may be different for each gas. Based on imposed boundary conditions, the integration of equation 3 will result in slightly different equations for different situations.

2.2.2 Nitrous Oxide

Even though N_2O is a sparingly soluble gas, N_2O is more soluble than O_2 or N_2 and has a 20 times larger Henry's coefficient in water than O_2 (Sander, 2015). Concentrations of N_2O in process air entering a wastewater aeration basin are usually below equilibrium with the dissolved concentration, so dissolved N_2O is typically stripped from the basin during aeration.

For mass transfer across a single bubble, Matter-Müller et al. (1981) proposed an adjustment to the basic mass transfer equation to account for the ratio of the surface area of a single bubble to the volume of gas in a single bubble.

$$V_B \frac{dC_G}{dt} = K_L * A_B * \left(C_L - \frac{C_G}{H}\right) \quad [4]$$

Where:
V_B = volume of gas within one bubble [m^3],
K_L = liquid-side mass-transfer coefficient [m/d], and
A_B = surface area of single bubble [m^2].

To account for mass transfer for all bubbles (n_b) within an aeration tank, the combined surface area of all bubbles and combined volume of all bubbles can be calculated using: $n * A_B = A_G$ and $n_b * V_B = V_G$. The following relationship can then be used:

$$\frac{A_B}{V_B} = \frac{aV_L}{V_G} \quad [5]$$

Where:
a = ratio of interfacial area to bulk liquid volume, A_G/V_L [m^2/m^3];
A_G = surface area of gas to liquid interface, in this case surface area of all bubbles [m^2];
V_L = volume of bulk liquid [m^3]; and
V_G = volume of gas within basin, in this case the volume of all bubbles [m^3].

Equation 4 can be combined with equation 5 and integrated to solve for the predicted off-gas concentration of N_2O for a known dissolved concentration. The alpha correction factor is included to emphasize the difference between clean water and wastewater, but in this case the beta factor for salinity is assumed to be negligible due to low salinity. To simplify the integration, C_L is assumed constant with respect to depth in the activated sludge basin. The latter assumption requires a well-mixed basin with no vertical stratification of dissolved N_2O concentrations. These simplifications allow for integration with regards to time from the bottom of the basin ($C_G = C_{G,in}$ and t = 0) to the surface ($C_G = C_{G,out}$ and t = bubble residence time, t, in days) to yield the following equations:

$$\frac{\partial C_G}{\partial t} = (\alpha) * K_L a * \frac{V_L}{V_G} * (C_L - \frac{C_G}{H}) \quad [6]$$

$$C_{G,out} = C_{G,in} * e^{-\frac{(\alpha)*K_L a*\frac{V_L}{V_G}*t}{H}} + H * C_L * \left(1 - e^{-\frac{(\alpha)*K_L a*\frac{V_L}{V_G}*t}{H}}\right) \quad [7]$$

Influent concentration can be assumed to be equal to ambient N_2O levels of approximately 330 ppb (NOAA, 2019). In cases of significant N_2O off-gas the influent N_2O can be excluded to simplify the equation, but it is recommended to confirm $C_{G,in}$ is truly negligible before

simplifying. It should also be noted that the K_La used in equations 6 and 7 is the K_La for N_2O.

The time of bubble residence, t, can be approximated by dividing the total volume of bubbles in the reactor (V_G) by the air flowrate (Q_A) in m^3/d (Matter-Müller, et al., 1981). Equation 7 then simplifies to:

$$C_{G,out} = C_{G,in} * e^{-\frac{(\alpha)*K_L a*V_L}{H*Q_A}} + H * C_L * \left(1 - e^{-\frac{(\alpha)*K_L a*V_L}{H*Q_A}}\right) \quad [8]$$

The Henry's coefficient is affected by temperature, the effects of which can be estimated within a limited temperature range using the Van't Hoff equation (Smith & Harvey, 2007).

$$H_{p/x} = H_{p/x\_0} * e^{\frac{\Delta H_{sol}}{R}\left(\frac{1}{T} - \frac{1}{T_0}\right)} \quad [9]$$

Where:

$H_{p/x}$ = Henry's coefficient in units of pressure [bar],
T = temperature [K],
H_{p/x_0} = Henry's coefficient at temperature T_0 [bar], and
$\frac{\Delta H_{sol}}{R}$ = temperature dependence term, equal to -2675 K (NIST, 2018).

The unitless Henry's coefficient, H, is needed for mass transfer equation 8, so $H_{p/x}$ in equation 9 can be converted to unitless H by substituting into equation 10 to create equation 11.

$$H = H_{p/x} * \frac{MW_{H_2O}}{\rho_{H_2O}} * \frac{1}{RT} \quad [10]$$

$$H = \left(H_{p/x\_0} * e^{\frac{\Delta H_{sol}}{R}\left(\frac{1}{T} - \frac{1}{T_0}\right)}\right) * \frac{MW_{H_2O}}{\rho_{H_2O}} * \frac{1}{RT} \quad [11]$$

Where:

MW_{H_2O} = molar mass of water [kg/mol],
ρ_{H_2O} = density of water [kg/L], and
R = ideal gas constant $\left[\frac{L*bar}{mol*K}\right]$.

The volumetric mass transfer coefficient is also temperature dependent. The temperature correction for K_La uses the Arrhenius equation where T_C is in Celsius, the given K_La is for 20 °C, and the unitless temperature conversion factor θ is typically 1.024 (ASCE, 2007).

$$K_L a_T = K_L a_{T=20C} * \theta^{(T_C - 20)} \quad [12]$$

The K_La for N_2O can be estimated from a known K_La for O_2 using equation 2, but if the K_La for O_2 is not known it is possible to calculate using dissolved and off-gas N_2O values if it is assumed that there is negligible change in dissolved N_2O with time (approximate steady-state conditions). In this case, the stripped N_2O can be divided by the concentration gradient and volume (Foley, et al., 2010):

$$K_L a = \frac{Q_A * C_G}{V_L * (C_S - C_L)} \quad [13]$$

Where:

C_S = saturation concentration of N_2O at operating temperature and pressure [mg/L].

Foley et al. (2010) measured liquid and off-gas N_2O in lab reactor experiments and from three WWTPs in Australia to develop a power law relationship equation for the mass transfer coefficient K_La. From their results, they proposed an empirical air flow and depth correction for the K_La value for N_2O:

$$K_L a_F^* = \left(\frac{d_R}{d_L}\right)^{-0.49} * \left(34500 * v_g\right)^{0.86} \quad [14]$$

Where:

$K_La^*_F$ = Field-determined N_2O volumetric mass transfer coefficient [d^{-1}];
d_L = depth of the lab reactor from which this equation was established, defined by Foley et al. as 0.815 m;
d_R = depth of the reactor the K_La is being solved for [m]; and
v_g = superficial gas velocity [$m^3/m^2/s$], equal to air flowrate (Q_A) in m^3/s divided by aerated area (A).

Due to this equation's empirical nature, units do not cancel. This K_La correlation was tested up to a depth of 5 meters and Foley et al. (2010) found a range of K_La values from approximately 20 to 100 d^{-1} at the three WWTPs. They also found approximate lab K_La values of 50 to 300 d^{-1} in wastewater and 100 to 400 d^{-1} in clean water, with a clear correlation between superficial velocity and K_La in lab and WWTP experiments.

2.2.3 Oxygen

Transfer of O_2 is crucial to aerobic wastewater treatment, and a significant portion of research has been dedicated to studying O_2 transfer in clean water and in wastewater. Because O_2 transfer is better understood than N_2O transfer, N_2O transfer is often considered to behave similarly to O_2 transfer. The basics of O_2 transfer also follow equation 3, and there is more knowledge of α and β factors values for O_2 in wastewater than for N_2O in wastewater.

In the case of O_2 transfer, it is desirable to transfer a large quantity of O_2 from process air to wastewater quickly in order to provide sufficient DO for aerobic bacteria. This oxygen transfer rate (OTR) is often expressed as (Metcalf & Eddy, 2011):

$$OTR = SOTR * \alpha * F * \left(\frac{\beta C_{\bar{S},T,H} - C_L}{C_{s,20}}\right) * 1.024^{(Tc-20)} \quad [15]$$

Where:

OTR = oxygen transfer rate [kg O_2/h];
SOTR = standard oxygen transfer rate in clean water at 20 °C [kg O_2/h];
α = correction factor for gas transfer rate in wastewater compared to clean water;
β = correction factor for maximum solubility in wastewater, typically 0.95-0.99 (Metcalf & Eddy, 2011);
F = aeration membrane fouling factor, typically 0.65-0.9 (Metcalf & Eddy, 2011);
$C_{\bar{S},T,H}$ = average clean water oxygen saturation at operating temperature and altitude [mg/L];
C_L = dissolved oxygen at operating conditions [mg/L];
$C_{s,20}$ = saturated oxygen at 20 °C and 1 atm [mg/L]; and
T_C = temperature in Celsius [°C].

The OTR can also be solved for with the following equation (Rosso, 2018):

$$OTR = \frac{1}{24} K_L a * (C_s - C_L) * V_L * 10^{-3} \quad [16]$$

Where:

K_La = liquid-side volumetric mass transfer coefficient for O_2 [d^{-1}];
C_s = saturated DO at operating temperature and pressure [mg/L];
V = Aerated tank volume [m^3];
10^{-3} is for unit conversion from mg*m^3/L to kg; and
$\frac{1}{24}$ is for unit conversion from d^{-1} to h^{-1} (not necessary if K_La in units of h^{-1}).

Oxygen uptake rate (OUR) is a measure of the rate of O_2 consumption, and changes in OUR can indicate changes in load. The OUR is included in equations 1 and 3 as the "r" term, or uptake rate. When DO remains constant with time, OUR can be calculated by dividing OTR by the volume (V) over which the OTR is applicable (Equation 17). The resulting units are in kg/m^3/h, but are commonly converted to mg/L/h.

$$OUR = \frac{OTR}{V} \quad [17]$$

The majority of energy costs for a WWTP using a traditional activated sludge process come from aeration (WEF, 2009). The energy sector and fuel combustion are responsible for 8-20 % of anthropogenic N_2O production. Electricity and heating are responsible for approximately 31 % of anthropogenic total greenhouse gas production, or 75 % of global emissions if fuel combustion is included (EPA, 2019; IPCC, 2013). Therefore, energy

savings can reduce the overall greenhouse gas footprint of a WWTP. Aeration efficiency (AE) and oxygen transfer efficiency (OTE) provide valuable information on the efficiency of an aeration basin, and can be calculated with the following equations (Rosso, 2018):

$$AE = \frac{OTR}{P} \quad [18]$$

$$OTE = \frac{OTR}{W_{O_2}} \sim \frac{O_{2,in} - O_{2,out}}{O_{2,in}} \quad [19]$$

Where:

AE = aeration efficiency [kg O_2/kWh],
P = power use of aeration [kW],
W = mass flow rate [kg/h], and
$O_{2,in}$ and $O_{2,out}$ are mole ratios of oxygen to inert gases in and out of the system, respectively [unitless].

3 Research Background

3.1 Viikinmäki Wastewater Treatment Plant

3.1.1 Overview

The Viikinmäki WWTP in Helsinki, Finland is currently the largest WWTP in the Nordics. Viikinmäki began operating in 1994 and serves a population of approximately 800 000 to treat an average of 270 000 m^3/d wastewater from 85 % residential and 15 % industrial sources (HSY, 2015).

Viikinmäki WWTP performs physical, chemical, and biological treatment of wastewater, as well as tertiary treatment in denitrifying filters. Inlet water is screened and undergoes grit removal, pre-aeration, and primary settling in one of nine treatment lines (Figure 3). Wastewater is then treated with traditional nitrifying and denitrifying activated sludge with concurrent phosphorus precipitation using ferrous sulfate ($FeSO_4$). Alkalinity in the activated sludge basin is controlled through lime ($Ca(OH)_2$) addition. The Viikinmäki WWTP is fully automated and aeration, flowrates, and chemical dosing are controlled using input from an array of sensors, chemical analyzers, and flowmeters.

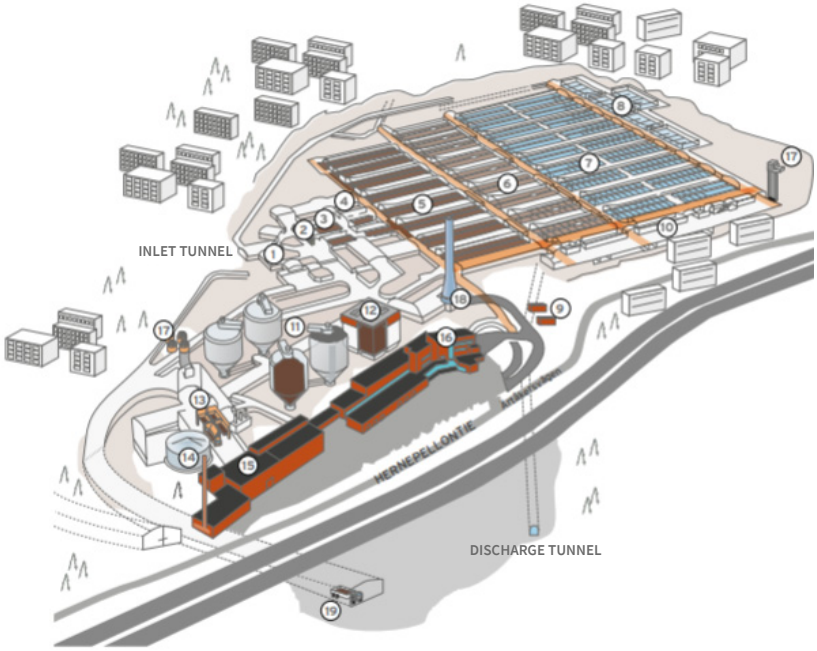

Figure 3. Layout of Viikinmäki wastewater treatment plant. (HSY, 2015)

Following nitrification and denitrification in the aeration basins, activated sludge settles in secondary clarifiers and is pumped back to the aeration basins as return activated sludge (RAS). Excess bacteria are wasted along with primary sludge from the primary sedimentation basin (Figure 4). Clarified wastewater flows from secondary sedimentation to the tertiary denitrifying biological filters, where methanol (CH_3OH) is added to promote microbial denitrification of any remaining NO_3^-. The entire Viikinmäki WWTP is underground, and outside air is circulated through the plant to maintain air quality. Process air from the aeration basins is incorporated into the circulated air, and all air from Viikinmäki WWTP exits from an outlet chimney that is continuously monitored (HSY, 2015).

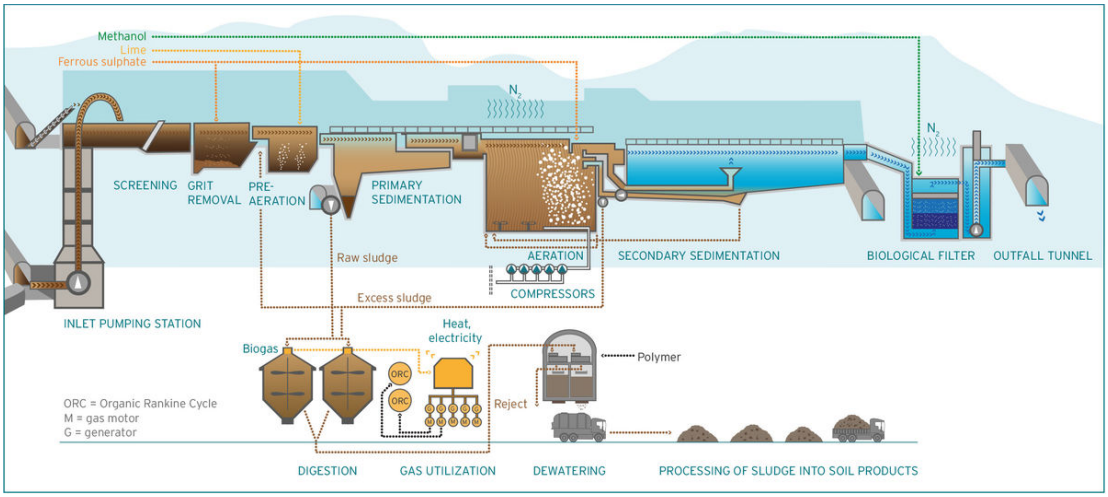

Figure 4. Treatment train at Viikinmäki WWTP (HSY, 2015).

To protect the Baltic Sea, which Viikinmäki WWTP discharges to through a pipeline extending 16 km from the southern shore of Helsinki, the Finnish ministry of the environment has set stricter water quality limits than the minimum limits outlined within the European Union water framework directive (EU, 2000 cited in Fred, n.d.; Oikeusministeriö, 2008). Viikinmäki consistently treats water to cleaner than the standards set by their discharge permit, as seen in Table 1.

Table 1. Permitted and discharged water quality parameters at Viikinmäki WWTP.

		EU WFD Limits	Viikinmäki Permit Limits	Viikinmäki Treatment Results 2017
BOD	concentration	30 mg/L	10 mg/L	4.3 mg/L
	reduction	70 %	95 %	98 %
COD	concentration	--[a]	75 mg/L	40
	reduction	--[a]	85 %	93 %
TN	concentration	10 mg/L	20 mg/L[b]	4.0 mg/L
	reduction	70 %	80 %	91%
TP	concentration	1.00 mg/L	0.30 mg/L	0.19 mg/L
	reduction	80 %	95 %	97 %

Notes: [a] *Data not listed.*
[b] *When process water temperature ≥ 12 °C, effluent TN must be below 20 mg/L (24-hour composite).*
Sources: Fred, n.d.; HSY, 2018

3.1.2 Activated Sludge Process

In each of the nine treatment lines, the activated sludge process is carried out in 11500 m^3 aeration basins split into six zones, three on each side of the central walkway, as well as a degassing zone prior to secondary sedimentation (Figure 5). Each basin is built within rock, so the side walls of the basin are rock walls from excavation and are inaccessible. The basins are aerated with fine-bubble diffuser arrays located at the bottom of all six zones, and aeration can be turned on and off individually for each zone. Under normal conditions, zones 1 and 2 are anoxic, zone 3 aeration turns on and off based on NH_4^+ loading, and zones 4 through 6 are continuously aerated. However, under poor nitrification conditions zones 2 through 6 may all operate as aerobic zones. The typical retention time in the activated sludge basin is 8 hours (HSY, 2015).

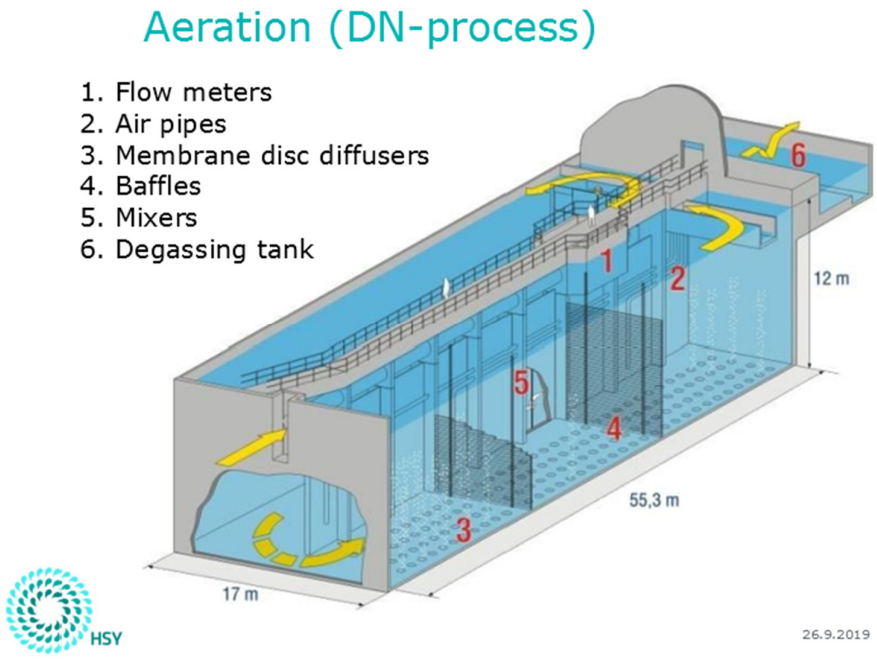

Figure 5. Layout of Viikinmäki aeration basins (HSY, 2019). Yellow lines indicate direction of water flow.

Aeration of zones is controlled by online NH_4^+ analysis that signal when the switching zones should begin aeration. The first threshold starts aeration in zone 3, while a second NH_4^+ concentration threshold begins aeration in zone 2. The air flow to each online zone is controlled by DO probes. The DO setpoint is adjustable, but for most of the measurement campaign it was set at 3.0 mg/L. Alkalinity is adjusted by adding $Ca(OH)_2$ when the online analyzed alkalinity falls below a set value. Phosphorus is chemically precipitated from wastewater at Viikinmäki using $FeSO_4$. The majority of $FeSO_4$ is added to the process before grit removal, but additional $FeSO_4$ is added to the degassing tank of the activated sludge basins. In 2015, Viikinmäki used 8268 metric tons of $FeSO_4$ and 2642 metric tons of $Ca(OH)_2$ (HSY, 2015).

3.2 Related Studies

3.2.1 Prior Nitrous Oxide Studies at Viikinmäki

Greenhouse gas research has been ongoing at Viikinmäki since 2007, and continuous online monitoring of greenhouse gases began in 2012 as part of HSY's efforts to reduce greenhouse gas emissions and to attain carbon neutrality in the Helsinki metropolitan area by 2050 (HSY, 2016).

In 2012, localized N_2O emissions were measured using a mobile FTIR analyzer (Gasmet Oy, Finland) on the activated sludge and secondary settling basins of six treatment plants in southern Finland including Viikinmäki (Leppänen, 2012). The findings from this study suggested that the production of N_2O from both activated sludge and secondary settling at Viikinmäki was not negligible. In 2013, local N_2O emissions were compared to the plant-wide emissions using the same mobile analyzer as in Leppänen's 2012 study and a continuous FTIR analyzer in Viikinmäki (Kosonen, 2013). The aim of the 2013 study was to better understand temporal variations in N_2O emission and see if a link between operating parameters and off-gas concentrations could be found. Conclusive links between water quality parameters and N_2O emission were difficult to make, but potential effects from nutrient loading and alkalinity were identified. Data from these two master's theses were included in later publications (Kosonen, et al., 2016; Mikola, et al., 2014).

In 2016, newly installed Clark-type N_2O microsensors (Unisense, Denmark) and Viikinmäki's off-gas N_2O monitoring (section 4.2.3) were used to generate a model to simulate production and emission of N_2O in Viikinmäki's activated sludge basins (Blomberg, 2016). This model captured the daily dynamics of N_2O emissions well, but N_2O emissions were consistently over-estimated and it was concluded that issues with the stripping model used in this N_2O model were leading to this over-estimation (Blomberg, et al., 2018).

Emitted N_2O concentrations from Viikinmäki's exhaust chimney ranged from 0 to 80 ppm in 2012 and 2013, with evidence of possible increased N_2O production during upsets in nitrification (Figure 6). However, Kosonen (2013) performed an analysis of variable correlation and did not find a strong correlation between nitrification and N_2O production. Average N_2O EFs of 0.77, 2.75, and 1.9 % of influent nitrogen were calculated for Viikinmäki in 2011 (Leppänen, 2012), 2012 (Kosonen, 2013), and 2013 (Kosonen, et al., 2016).

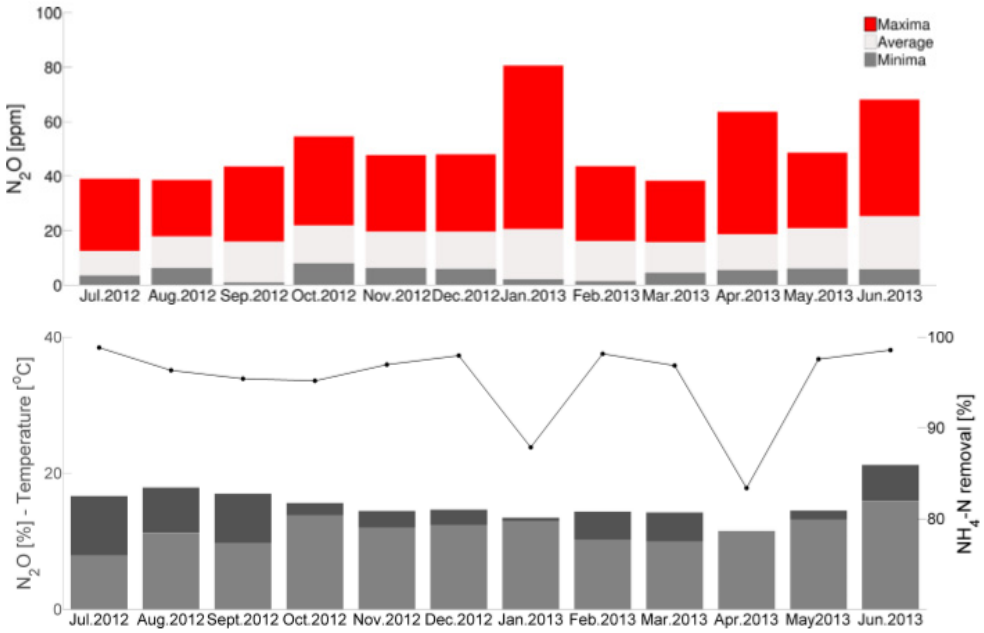

Figure 6. Annual variations in wastewater temperature and N_2O production at the Viikinmäki WWTP in July 2012-June 2013 (Kosonen, et al., 2016). Upper graph represents maximum, minimum, and average N_2O emissions. Lower graph represents average values for monthly N_2O emissions (light gray), temperatures (dark gray), and nitrification performance as percent NH_4-N removal (solid line).

3.2.2 Global Research

There have been a significant number of studies dedicated to better understanding and quantifying the off-gas of N_2O from WWTPs worldwide (see section 2.1). There have been fewer studies where both the dissolved and gaseous N_2O are measured concurrently, with key examples that have already been mentioned in section 2.1.2 including Kampschreur et al. (2008), Foley et al. (2010), Ahn et al. (2010a), and Yu et al. (2010). There are no known studies which combine simultaneous dissolved and off-gas N_2O measurements with O_2 transfer measurements.

Chandran outlined a protocol for measuring N_2O flux (2011) that includes a method of measuring off-gas and dissolved N_2O from the same location, but no published method was found for measuring O_2 transfer from the same location as N_2O flux. There is little published on the exact relationship between dissolved and emitted N_2O within wastewater treatment, and dissolved N_2O is often assumed to behave similarly to dissolved O_2. The studies with closest agreement between liquid and gas measurements are based on grab samples, tested *ex situ* with a gas chromatograph (Schneider, et al., 2015; Townsend-Small, et al., 2011).

Baresel et al. (2016) calculated N_2O emissions to the environment at an enclosed WWTP in Sweden using dissolved N_2O probe readings (Clark-type microsensor, Unisense, Denmark). In their study, they compared the calculated values to measured plant-wide emissions and found good agreement between the predicted and measured off-gas N_2O. Baresel et al. also performed a sensitivity analysis of their results and found liquid N_2O concentrations to be

the most sensitive variable in prediction of N_2O off-gas, while variability in temperature and reactor dimensions had a lesser impact on calculation results.

Bellandi et al. (2018) measured dissolved and off-gas N_2O during 24-hour sampling periods at two of three WWTPs where they took measurements, and their data showed that dissolved and emitted N_2O had similar temporal variation within the time period measured. However, N_2O stripping was not quantified and the measured time period was too short to conclude the same trends would be consistently observed.

4 Materials and Methods

4.1 Measurement Campaign

Data were collected from the activated sludge basins in lines 5 and 9 at Viikinmäki WWTP in Helsinki, Finland between 2 April and 1 July 2019, with continuous off-gas measurements occurring during a two-week period from 7 to 20 May.

Continuous off-gas monitoring using a floating hood assembly (described in section 4.2.2) occurred from 7 to 20 May in zones 4, 5, and 6 of the aeration basins in lines 5 and 9. Off-gas monitoring was intended to compare local dissolved and off-gas N_2O concentrations as well as to compare N_2O and O_2 transfer. Off-gas data were supplemented with online operational data from Viikinmäki (section 4.2.3). Measurement of dissolved N_2O at various depths in order to determine if there was vertical N_2O stratification in the basins was performed on 2 April in line 5 zone 4, and a second time on 1 July in line 9 zone 6.

During this measurement campaign, the Viikinmäki WWTP was experiencing an unprecedented increase in N_2O production that began around the start of April 2019. Dissolved and off-gas N_2O concentrations were significantly higher than the average concentrations recorded since the start of continuous greenhouse gas monitoring in 2012.

4.2 Equipment

4.2.1 Dissolved Measurements

Dissolved N_2O was measured using online Clark-type microsensors (Unisense, Denmark) that were installed in zones 4 and 6 of lines 5 and 9 (Figure 7 and Figure 8). These sensors are calibrated every 2 months during normal operation at Viikinmäki and had been calibrated prior to continuous measurements. For the N_2O depth profile, a Ruttner sampling device was used to grab samples from set depths as outlined in section 4.3.2.

Figure 7. Clark-type microsensor N_2O probe (Unisense, n.d.).

Figure 8. Both line 9 N_2O probes in the same zone, a placement typically used to confirm probe calibration.

Two DO probes, a YSI 550A and a Hach LDO103, were used alternately to record local DO concentrations and temperature during manual O_2 transfer tests.

4.2.2 Off-Gas Measurements

A modular off-gas hood made of four plastic containers with inner dimensions of 36 x 56 x 28 cm and outer dimensions of 40 x 60 x 28.5 cm was constructed at the Aalto University Water Laboratory in Espoo, Finland (Figure 9). This design was based on modular off-gas hoods used by Rosso in previous off-gas tests (Rosso, 2018). The plastic containers were secured together and headspaces connected with 50 mm rubber ring joint polypropylene pipes. Connections were reinforced and sealed with duct tape. The external surface area of the hood was roughly 1 m^2 and the internal surface area was just over 0.8 m^2. Gas was directed from the hood to a measurement array via 20 meters of 38 mm flexible PVC tubing.

Figure 9. Modular off-gas hood on Viikinmäki walkway.

Due to significant turbulence on the surface of the aerated basins, the off-gas hood was only deployed near the central walking path (Figure 16, section 4.3.1). In line 9, a previously installed Alphameter (INVENT, Germany) with a net surface intake of 1 m^2 was used to take measurements 2.5 m from the walkway (Figure 10). The Alphameter was connected to the measurement array via approximately 20 m of 16 mm ID PVC tubing.

Figure 10. Off-gas hood and Alphameter hood in place in zone 4 of line 9 at Viikinmäki.

At the mobile measurement array (Figure 11), a hot wire thermos-anemometer with datalogging capabilities (Extech; Nashua, NH) measured gas velocity and temperature (Figure 12). Downstream of this, a Gasmet DX4015 Fourier Transform Infrared (FTIR) analyzer pulled a 2 L/min sample from the collected gas, heated it to 50 °C, and performed FTIR spectroscopy analysis. The Gasmet analyzer was controlled by Calcmet software (Gasmet Oy, Finland), and had a spectrum library set up using reference samples to calculate for N_2O, NH_3, CO_2, carbon monoxide (CO), methane (CH_4), and hexane concentrations. The DX4015 was calibrated daily with grade 5.0 pure N_2 to create a zero background.

After the Gasmet intake, an additional 0.94 L/min of sample was pumped through a desiccating column containing a mixture of orange and brown indicating silica gel desiccant (Disidry Silicagel, Italy) for water vapor removal and sodium hydroxide (NaOH) pellets for CO_2 removal. This provided a dry sample for the O_2 analyzer (AMI Model 65; Fountain Valley, CA) to measure the percent O_2 in the off-gas sample. An external datalogger (squirrel meter/logger 1000 series; Grant Instruments, UK) recorded percent O_2 in between manually recorded off-gas tests (Figure 13).

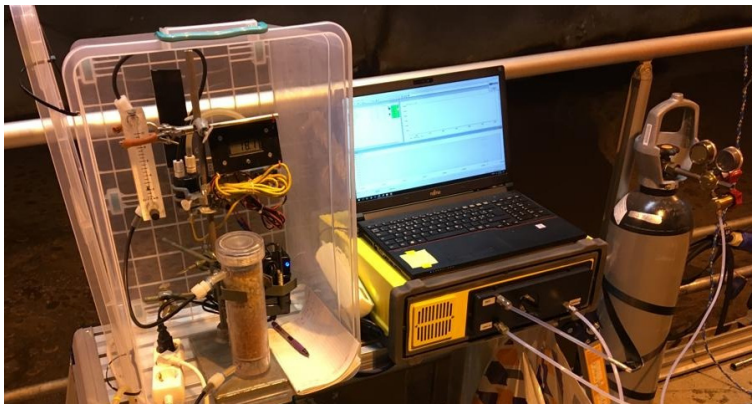

Figure 11. Mobile gas measurement array. From left to right: O_2 measurement equipment enclosure (see Figure 13), laptop with Calcmet software seated on Gasmet analyzer, and grade 5.0 N_2 gas cylinder for calibration. Photographed by Diego Rosso, 2019.

Figure 12. Hot wire thermos-anemometer in sample inlet pipe, located under components in Figure 11.

Figure 13. Off-gas O_2 measurement equipment. Sample is drawn through a desiccant column and flowmeter, then through an AMI O_2 analyzer connected to a read-out. Datalogger at bottom right.

4.2.3 Online Data and Laboratory Analysis

Operational data are continuously collected at Viikinmäki using an array of sensors and analyzers. The locations of sensors and analyzers in the activated sludge basin is shown in Figure 14. Flowmeters across the plant measure aeration air per zone in the activated sludge basins, total exhaust air, and wastewater flow entering and exiting the plant as well as in each treatment line.

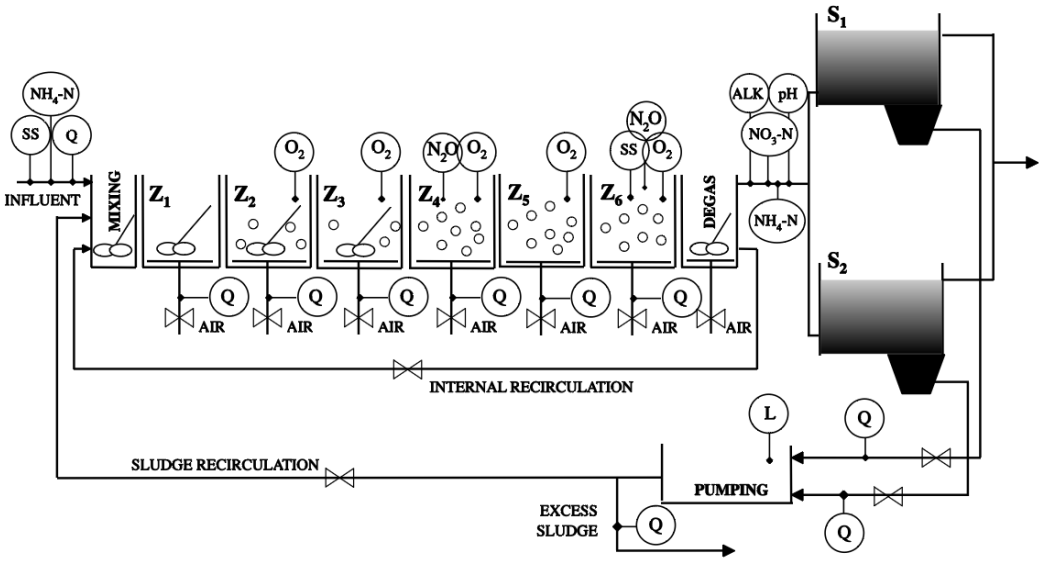

Figure 14. Linear layout of activated sludge process with location of online measurements (modified from Haimi, 2016). ALK = alkalinity. SS = Suspended solids. L = Level sensor.

Exhaust air is monitored with a Gasmet CEMS II FTIR analyzer with Calcmet software that provides continuous emissions data for CH_4, N_2O, CO_2, NO, NO_2^-, and NH_3 gas (Figure 15). The CEMS is automatically calibrated daily with grade 5.0 N_2.

Figure 15. Gasmet continuous emissions measurement system at Viikinmäki WWTP (Maja, 2018).

Twice per week, laboratory analyses are performed on 24-hour flow-based composite samples from multiple key locations at Viikinmäki. Within this thesis, laboratory analyses were used for calculating the average nitrification rate and EF during the measurement campaign.

4.3 Data Collection

4.3.1 Nitrous Oxide and Oxygen Transfer

Off-gas data collection began 7 May from the line 5 aeration basin. Multiple measurement locations were selected in order to compare gas transfer across the zones. However, high turbidity in zone 4 made off-gas measurements in this zone difficult. On 13 May, the off-gas hood and gas measurement array were moved to the line 9 aeration basin. In line 9, off-gas sample locations were selected based on proximity to dissolved N_2O probes. A map of the gas measurement and N_2O probe locations is shown in Figure 16.

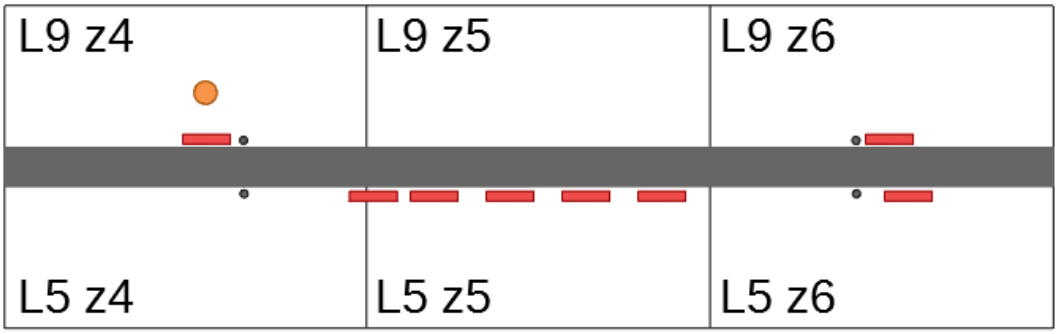

Figure 16. Off-gas hood measurement locations in lines 5 and 9. Line 9 zones are approximately a mirror image of the zones in line 5, so the two were super-imposed with the dark center as the walkway. Orange circle represents Alphameter location, red boxes are hood placements, and small gray circles are N_2O probes.

During gas collection, the off-gas hood was secured to the walking path railing with rope, preventing movement more than 1 m from the measurement location. The bottom of the hood was submerged to prevent intake of ambient air instead of exhaust gas from the basin. The pipes at the top of the gas hood were kept above the water level, although splashing of wastewater and foam across the top of the hood was a common occurrence.

The mobile FTIR analyzer recorded data every 1 minute, while dataloggers for velocity, off-gas temperature, and percent O_2 recorded values every 5 minutes. Brief interruptions to the logged data were necessary in order to move the off-gas hoods and calibrate equipment, but longer gaps also occurred as a result of battery death in the datalogger and an unidentified communication error with the FTIR analyzer for 24 hours on 11-12 May.

The mass load of N_2O emissions for Viikinmäki was calculated using the CEMS-II N_2O off-gas measurements and exit air flowrates. This was compared against the mass load of influent TN based off the average laboratory TN values multiplied by the average influent flowrate. Influent flowrate was not available, so the effluent flowrate was used under the

assumption that it is approximately equal. The EF was calculated as follows:

$$EF = \frac{C_{N_2O-N,eff} * Q_{A,eff}}{C_{TN,inf} * Q_{WW,eff}} \quad [20]$$

Where:

$C_{N2O-N,eff}$ = nitrous oxide concentration in exit air as nitrogen [kg-N/m^3],
$C_{TN,inf}$ = influent wastewater total nitrogen [kg-N/m^3],
$Q_{A,eff}$ = exit air flowrate [m^3/s], and
$Q_{WW,eff}$ = effluent wastewater flowrate [m^3/s].

4.3.2 Nitrous Oxide Vertical Profile Measurements

The Unisense dissolved N_2O microsensors can be submerged to 5 m depth, but their accuracy is not guaranteed at greater depths. Two experiments were performed to compare N_2O concentrations in the top 5 meters of the aeration basin and to test the feasibility of measuring N_2O from a Ruttner sampler. In the first test on 2 April 2019, the Unisense dissolved N_2O probe in zone 4 of line 5 (N_2O probe 1) was lowered to two set depths (3 and 5 m). After probe 1 was lowered to each depth, it was removed and a Ruttner sampler was then lowered to the same depth. The Ruttner sampler was then closed and removed, and the drawn sample was measured with probe 1 by opening the top lid of the Ruttner but leaving the bottom lid closed (Figure 17). N_2O values were compared using the nearby Unisense Environment screens. Separate pH measurements were taken from the Ruttner sampler earlier in the day in zones 1 and 6 of lines 5 and 9, at depths of 0, 4, 6, and 8 meters.

The experiment was repeated on 1 July 2019 in line 9 zone 6. A different probe of the same model (N_2O probe 2), informally regarded as the most reliable probe by Viikinmäki staff, was used to measure dissolved N_2O. In this repeat test, the Ruttner sampler and Unisense probe were lowered at the same time to the same depth (1, 3, or 5 meters). Once probe 2 gave a stable reading, both the Ruttner and probe 2 were removed and probe 2 was used to measure from the Ruttner using the same procedure as during the first experiment. The pH of each depth was measured with a WTW 3110 pH meter from Aalto University. Each depth was measured in duplicate. Values were checked from the screens and online N_2O probe data was obtained for the test period.

Figure 17. N_2O probe submerged in Ruttner sampler. Left: 2 April test. Right: 1 July test, pH and N_2O probes.

4.4 Data Analysis

Continuously measured data were consolidated into 5-minute averages and erroneous values were removed. Removal of erroneous values occurred first by deleting impossible values (temperature readings under 5 °C or over 25 °C and dissolved gas readings above the solubility limit or below zero) and values from times when it was known the probes were being moved or calibrated. The data were then reviewed again by comparing with 3 standard deviations. Outliers were removed except when more than two consecutive outliers were flagged, in which case a 6 standard deviation outlier check was run instead. The purpose of outlier removal was to remove false readings, not to normalize the dataset, so in most cases the decision was made to err on the side of keeping slightly erroneous data rather than accidentally removing true minimum and maximum values.

Data from the FTIR analyzer were sent to Gasmet for review against standards to ensure accuracy. Gasmet data was initially measured on a 1-minute interval, so average values were calculated for all data within the established 5-minute intervals. Only data that had been affected by the daily calibration or by a known communication error were removed.

Logged datasets for velocity and O_2 concentrations had to be reviewed against field notes, as periods of loss of power had affected the date stamp. After review, all data were assigned to within 10 minutes of their true collection time.

In order to compare data sets, it was necessary to minimize the number of data gaps. For data gaps under 20 minutes (4 contiguous blank spaces), including those created by deleting erroneous values, approximate values were extrapolated based on the preceding and following values using the equation below. In cases where data gaps were larger than 20 minutes or the data could not be extrapolated due to no preceding or following data from the same measurement location, the gaps were left.

$$x_n = \frac{\sum_{i=j+1}^{k+1}[x_{n-i}]+\sum_{i=k+1}^{j+1}[x_{n+i}]}{j+k+2} \quad [21]$$

Where:

x_n = blank value to fill,
j = number of blank values preceding x_n, and
k = number of blank values following x_n.

Unknown constants in calculations were estimated using the Microsoft Excel Solver add-in evolutionary method, with constraints, to minimize the sum of the absolute error between calculated and measured values at each time.

5 Results and Discussion

5.1 Method for Simultaneous Measurement

For this study, a novel method of off-gas measurements for N_2O and O_2 concentrations alongside flow metering and dissolved concentrations from Viikinmäki's online data was used to compare N_2O and O_2 transfer. The hood and measurement array were mobile and could be left to log data autonomously with a single calibration and visual inspection every 24 hours. This method performed well and could be improved upon for future applications.

The off-gas hood for this study was well-designed for capturing gas above aeration basins. The hood surface area (0.81 m^2) was sufficient to measure 0.5 % of the surface area of the Viikinmäki basin per selected location, reducing the number of sampling locations required for representative sampling compared to smaller hoods. Large diameter tubing from the off-gas hood allowed gas to travel to the measurement array with insignificant pressure losses and minimal lag between sample collection and measurement. This same hood would not work for sampling basins with minimal gas production. For measurements of such basins a sample hood with a sweep gas, as in Chandran's protocol (2011), would be recommended.

The measurement array was highly effective for measuring gas flow as well as O_2 and N_2O concentrations. This array depends on a constant power supply in order to take continuous samples, so for long periods of time when the array is unmanned it is recommended to use a continuous power source such as wired power. The array and hood could be moved by two people within a reasonable time frame, but mobility could be further improved if the analyzers were attached to a rolling cart instead of a stationary bench. A smaller gas cylinder for N_2 calibration would also increase mobility.

Dissolved measurements from directly next to the hood are preferable over measurements from elsewhere in the same zone, so deploying probes next to or even possibly attaching them to the gas hood would improve data quality (Figure 18).

Figure 18. Off-gas hood in place between DO probe (left, downstream by less than 1 m) and two N_2O probes (right, farthest probe upstream by less than 1.5 m).

The off-gas hood could be improved further by increasing durability and would likely perform better in WWTPs with less surface turbulence. Measurements in the middle of zones is possible in WWTPs with access to both sides of the zone, but within Viikinmäki where basins are enclosed within rock tunnels a different method of deployment would be necessary to reach the center.

5.2 Vertical Profiles

Off-gas N_2O calculations depended on the assumption of a vertically well-mixed basin, so vertical profiles of lines 5 and 9 were performed on 2 April and 1 July in order to assess variation of N_2O concentrations with depth.

On 2 April, the measured N_2O at both depths in the basin and from the Ruttner showed a difference of up to 0.02 mg/L dissolved N_2O However, the 1 July N_2O values showed significant differences between the in-basin and Ruttner samples. Samples measured in the Ruttner sampler continuously increased in N_2O concentration due to continued biological N_2O production and a lack of aeration that resulted in a lack of N_2O stripping. This same result was seen in all tests at all depths on 1 July, as shown in Figure 19 on the following page. In contrast, the total difference for the in-basin N_2O probe readings at different depths was less than 0.03 mg/L, or within ± 8 % difference (Table 2).

Table 2. Unisense N_2O readings and depths.

Date and locations	Depth[1]	Ambient N_2O reading[2]	Ruttner N_2O reading[2]
2 April, line 5 zone 4	3 m	0.11 mg/L	0.10 mg/L
	5 m	0.10 mg/L	0.09 mg/L
1 July, line 9 zone 6	1 m	0.36 mg/L	*
	3 m	0.37 mg/L	*
	5 m	0.39 mg/L	*

Notes: *1. Combined errors in depth marking accuracy and low visibility of depth markings led to an uncertainty of approximately ± 0.5 meters.*
2. Values were recorded when readings appeared stable (very gradual or no change). For 1 July Ruttner readings, no stable value was reached.
Using probe 1a (L5) and probe 2a (L9).

In addition to the N_2O measurements, pH measurements were also taken on 2 April and 1 July from multiple depths. Measurements of pH on 2 April had a maximum variation of 0.4, with no clear trend of increasing or decreasing pH with increasing depth. On 2 July, the measured pH did not change significantly between depths of 1 m and 5 m, with less than 0.02 difference. A table of pH measurements is available in Appendix 1.

The pH probe was successfully calibrated to pH 4 and 7 less than four hours before measurements were taken on each date, with almost no calibration drift occurring, though there was some concern about probe integrity due to the temperature reading on the pH probe being up to 3 °C higher than on the N_2O probes in the same basin.

On the final 2 July measurement from a depth of 5 m, the N_2O probe remained in the Ruttner sampler for over half an hour and the increase of N_2O was measured. There was occasional gentle mixing of the Ruttner to re-suspend the sludge blanket and ensure more accurate readings. Online data from this extended period of measurement was analyzed and N_2O production was found to be 121 ppm/d, or 0.084 ppm/h (Figure 19).

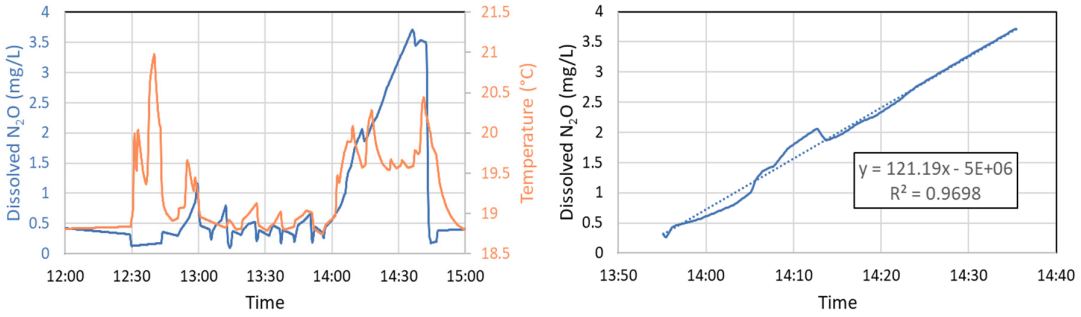

Figure 19. Vertical test N_2O probe trends. Left**:** all provided data. Elevated temperatures occur when probe is in the air or the Ruttner sampler. Right: trendline for N_2O production during last measurement from the Ruttner sampler. Decrease in N_2O occurred after gently mixing Ruttner sample with probe.

The attempted method for measuring potential vertical stratification of N_2O was not useful for depths below 5 m, so collected data from the top 5 m of the basin were used to make assumptions about the remaining basin depth. Although some variation was observed in the activated sludge basin across the first 5 m, the results of the vertical profiles suggest that total variation in N_2O across the depth of the activated sludge basins would be less than 20 %. So long as this variation is consistent over time, a site-specific model will be able to adjust for variation and the assumption of a vertically well-mixed basin should not introduce unacceptable error. The impact of uncertainties in dissolved N_2O is further considered in the sensitivity analysis in section 5.8.

5.3 Oxygen Transfer

Transfer of O_2 at Viikinmäki was measured in order to compare O_2 and N_2O transfer so that assumptions about similarity could be assessed and so that an N_2O K_La value could be estimated based on O_2 K_La values. Percent O_2, temperature, air flow rate, and DO were used to calculate the OTE, OTR, OUR, and mass transfer coefficients in the measured locations of the activated sludge basin. The O_2 transfer varied with location as well as with time. Results of all manually recorded O_2 tests can be seen in Table 3. Data were collected from sampling locations shown in Figure 16 in section 4.3.1.

Table 3. Average OTE, OUR, OTR, and $\alpha K_L a$ for all manually recorded measurement periods.

Date	Time Range	Position, Distance[1] (m)	OTE (%)	OUR[2] (mg/L/h)	OTR[2] (kg/h)	$\alpha K_L a$[2] (1/d)	Airflow[2] (m^3/h)
7-May	15:05-15:35	5.5, 22	27.2	43.8	82.3	91	1186
8-May	11:40-12:10	5.5, 30	29.1	47.0	88.3	99	1188
8-May	12:35-13:00	5.5, 26	28.7	46.1	86.6	97	1182
8-May	13:20-13:55	5.5, 22	25.9	42.0	78.9	88	1193
9-May	10:30-11:05	5.6, 47	28.7	20.1	37.7	42	513
9-May	15:30-16:00	5.5, 34	31.3	47.2	88.7	99	1110
10-May	13:05-13:25	5.4/5*, 19	13.9	30.8	57.9	63	1639
10-May	13:40-14:05	5.5, 22	22.1	41.7	78.4	88	1391
13-May	12:30-13:25	5.6, 47	31.3	23.7	44.6	50	557
14-May	11:20-13:55	9.4, 10	15.7	29.1	54.9	60	1370
16-May	12.30-14:20	9.4, 10	14.1	31.2	58.7	67	1636
16-May	12:40-14:50	9.4, 10α	12.4	27.4	51.6	59	1636
17-May	11:10-12:45	9.6, 46	24.1	27.4	51.4	59	835

Notes: *1. Written as Line.Zone, followed by distance. Distance is measured from the beginning of the walkway in zone 4, but zone 4 extends a few meters past the walkway. The Greek α is used to denote measurements from the Alphameter.*
2. Air flows for OUR, OTR, and mass transfer calculations are the measured aeration flowrates from Viikinmäki WWTP. Calculations from hood flowrates can be found in Appendix 2.
** This measurement was likely taken over the submerged baffle wall between zones 4 and 5.*

In general, OTE was highest in later zones and lowest in earlier zones. Air flowrates were higher in earlier zones, leading to larger bubbles and therefore lower surface area to volume ratios at the liquid-gas interface and lower OTE (EPA, 1989). However, increased air flow also increases turbulence and increases the non-volumetric mass transfer coefficient, K_L (Eckenfelder & Ford, 1968., cited in Rosso & Stenstrom, 2006).

There was daily variation in OTE for all lines and zones. The lowest value from line 5 testing was from 10 May when the position in zone 5 at 22 m had an OTE of 22.1 % compared to the average of 26.6 % from the first 2 days of testing. In line 9 zone 4, the average OTE was 14.1 % for off-gas samples taken near the walkway and 12.4 % from the Alphameter hood approximately 2.5 meters from the wall. This difference was observed consistently in all three tests, which alternated between the floating off-gas hood and Alphameter hood with duplicate samples and sufficient time between runs for three full turnovers of tubing air. It therefore seems unlikely that this was a random error. The difference in OTE could be associated with diffuser positioning, unequal air flow across the width of zone 4, or possibly the effect of greater biomass growth on walls near the walking path.

Kinetics of O_2 transfer depend on a combination of airflow, uptake, and transfer efficiency. The OTR and $\alpha K_L a$ were highest in locations with high OTE and airflow (i.e. 8 and 9 May

in zone 5 of line 5) and lowest in locations with low OTE and airflow. However, the lowest OTEs were usually connected to higher airflows. Reduced OTR and αK_La values were therefore seen either in locations with low OTE (zone 4/5 baffle in line 5) or in locations with low airflow (zone 6 of line 5). In these cases, air flow had a greater effect on the mass transfer coefficient and transfer rate than transfer efficiency.

The Alphameter tubing has a smaller diameter than the off-gas hood, 16 mm compared to 38 mm. As a result, less air flowed through the Alphameter tubing and the sample flowrate was not representative of the zone's total air flow. Therefore, calculations for OUR, OTR, and mass transfer coefficients were made using the plant's zone air flows. A comparison of O_2 transfer values based on hood and zone measurements can be found in Appendix 2.

Continuous measurements of percent O_2 and plant operational data were used to track changes in OTE, OTR, and mass transfer coefficients over time (Figure 20). Within zone 4 of line 9, there was a clear diurnal pattern of reduced mass transfer overnight that closely followed the flowrate of air to zone 4.

It is common to report OTE values in percentage O_2 transfer per depth of diffuser submergence. The range of OTE measured during this period was 1.1 %/m to 2.6 %/m from the manual measurements and 0.75 to 2.1 %/m in the continuous measurements. Under clean water conditions at 20 °C, the expected standard OTE (SOTE) for fine pore diffusers is between 6 and 7.5 %/m (WEF, 2017). Observed OTE in wastewater is more typically in the range of 1.5 to 4 %/m (EPA, 1999; Rosso, 2018). The manually measured OTEs therefore fall on the lower end of average ranges, while continuous OTE values would be considered very low. The continuous values were taken from zone 4, where OTE values were lowest, so these low values are not representative of the entire activated sludge basin.

The average alpha value can be determined using a known SOTE value for the diffusers alongside experimentally determined OTEs. In this case, based on average SOTE values for fine pore diffusers and the observed OTE values, the aeration alpha values observed were within the range of 0.1 and 0.4. These values are again on the low end compared to expected values of 0.4 to 0.8 for submerged diffusers (Metcalf & Eddy, 2011).

Based on the aeration alpha values of 0.1-0.4 and the calculated αK_La values for O_2 transfer, the O_2 K_La values would be approximately between 200 and 400 d^{-1}. Because the K_La is affected by so many different parameters, as discussed in section 2.1, it is difficult to compare between basins. However, in a thesis work by Hu (2006), fine pore diffuser clean water K_La values ranging from 120 to 600 d^{-1} were experimentally determined. Similarly, fine pore diffusers are often associated with K_La values between 125 and 220 d^{-1} (Painmanakul, et al., 2005). The estimated Viikinmäki K_La values are therefore likely within the range of reasonable values.

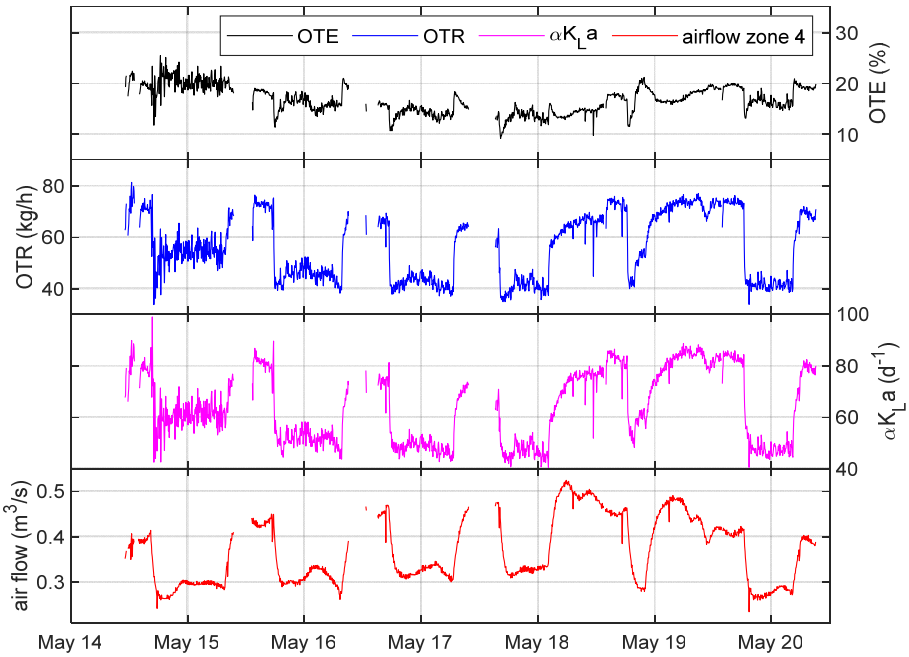

Figure 20. Continuous OTE, OTR, $\alpha K_L a$, and air flow rates in zone 4 of line 9.

On Saturday 18 May the OTR and air flow did not follow the same trend as closely as on other days. This observation occurred during an OTR peak that was often missed due to daily calibration, so it is also unclear if this deviation occurred daily or only on the 18th and 19th. Weekly laboratory analyses did not sample from this specific time period, and the only noticeable difference in online water quality on this day was a slight second ammonium and nitrate/nitrite peak that was more distinct than on other days (Figure 21).

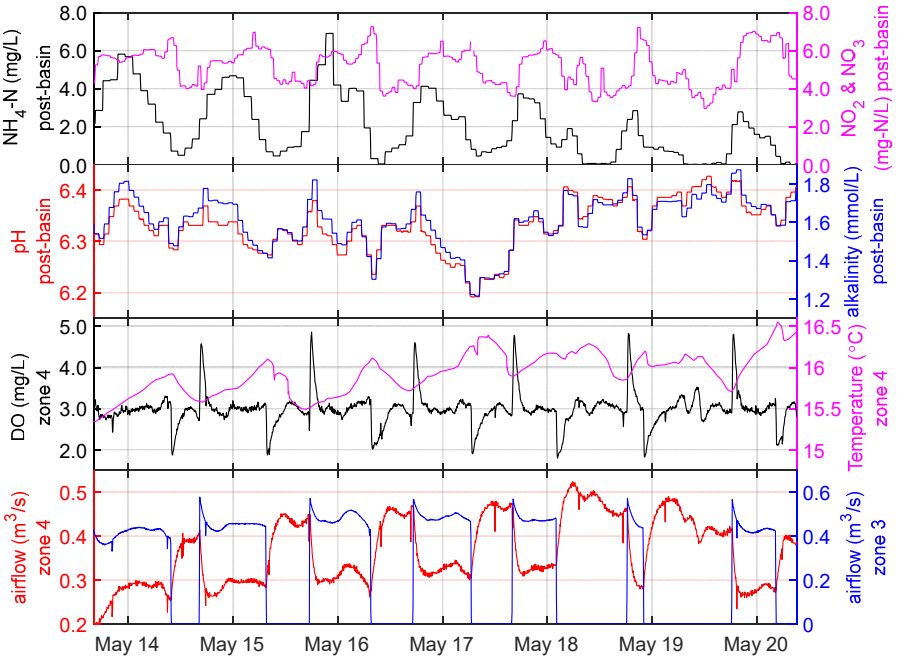

Figure 21. Continuously monitored water quality parameters in line 9 during 14.5.-21.5.2019. Post-basin values were measured via automated chemical analyses drawn from the effluent to the activated sludge process.

It is worth noting that the pH in Viikinmäki's activated sludge basins is lower than typical values of 7-8 in nitrification systems and 6.5-7 in denitrification systems (Metcalf & Eddy, 2011). This was also seen in pH probe measurements in zones 4 and 6 of lines 5 and 9 (Appendix 1). However, effluent alkalinity is not particularly low compared to recommended minimum values of 0.5 mmol/L. The DO setpoint is also safely above the typically recommended minimum of 2 mg/L (Metcalf & Eddy, 2011).

Continuous data were calculated using Viikinmäki's recorded air flows, DO, and N_2O probe temperature data for zone 4. Reference O_2 values were taken less often than during manually recorded O_2 transfer measurements. The continuous data may be slightly less accurate as a result, but the integrity of daily and weekly variation was not affected as all measured O_2 values would be equally impacted.

5.4 Nitrous Oxide Transfer

Dissolved and emitted N_2O were measured simultaneously to try to determine mass-transfer coefficients for stripping kinetics and to compare against O_2 transfer from the same time period. In all measured locations, the diurnal variation in dissolved N_2O closely matched the diurnal variation in N_2O emissions from the same location. Line 5 conditions had begun to stabilize after a period of exceptionally high dissolved N_2O concentrations. Line 5 conditions were more similar to regular conditions compared to line 9, which was experiencing incomplete nitrification and much higher dissolved and emitted N_2O.

In line 5, N_2O emissions were measured further from the dissolved N_2O probes. The majority of N_2O emissions were measured from zone 5, while N_2O probes were located in zones 4 and 6. Diurnal variation in dissolved and off-gas N_2O for line 5 was therefore compared against the averaged N_2O readings from the 4^{th} and 6^{th} zone (Figure 22). Due to the distance between liquid and gas measurement location, as well as the shorter measurement periods, it was difficult to estimate N_2O transfer in line 5. In line 9, the majority of N_2O off-gas measurements were within 4 meters distance from a dissolved N_2O probe, so emitted N_2O was compared against dissolved N_2O from the same zone (Figure 23). Because measurements were from the same location and the measurement period was longer, data from line 9 were used for N_2O transfer calculations. The higher N_2O production and emission in line 9 during the measurement period resulted in more distinct changes in N_2O concentrations compared to line 5.

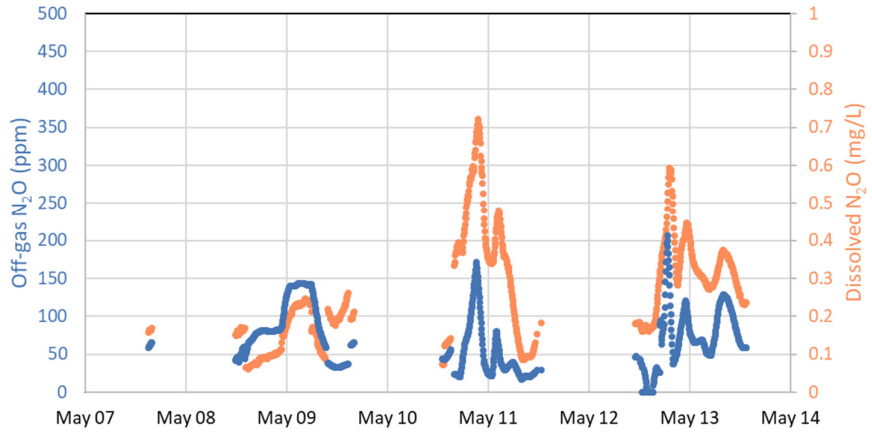

Figure 22. Dissolved and emitted N_2O concentrations for line 5. Sudden changes in off-gas N_2O values indicate movement of the off-gas hood to different zones. Dissolved N_2O readings are taken from the probe in the same location or, in the case of zone 5 measurements, an average of zone 4 and zone 6 readings.

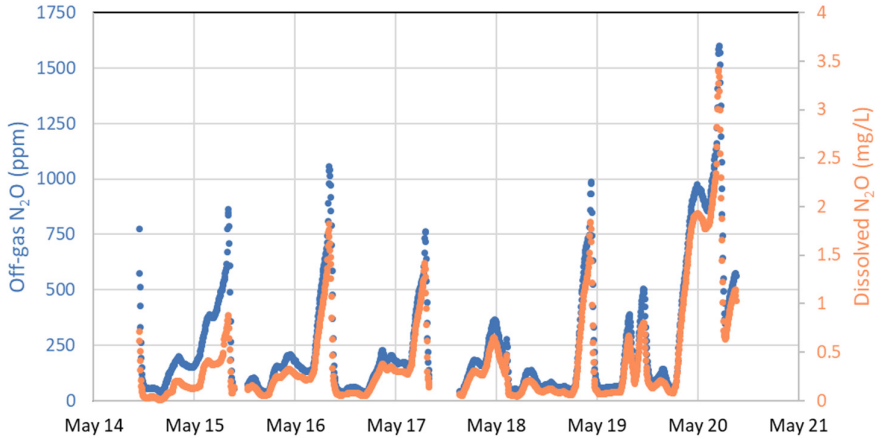

Figure 23. Dissolved and emitted N_2O concentrations for zone 4 of line 9. N_2O probes were moved on 15 and 17 May.

In both lines, zone 6 dissolved N_2O was consistently higher than zone 4 N_2O (Figure 24). It is clear that N_2O is produced in the aerobic zones of the activated sludge basins at Viikinmäki, with accumulation of N_2O leading to these increased concentrations in zone 6. This does not rule out additional anoxic zone production, but prior research at Viikinmäki has shown that N_2O production in anoxic zones is less significant than in aerobic zones (Leppänen, 2012).

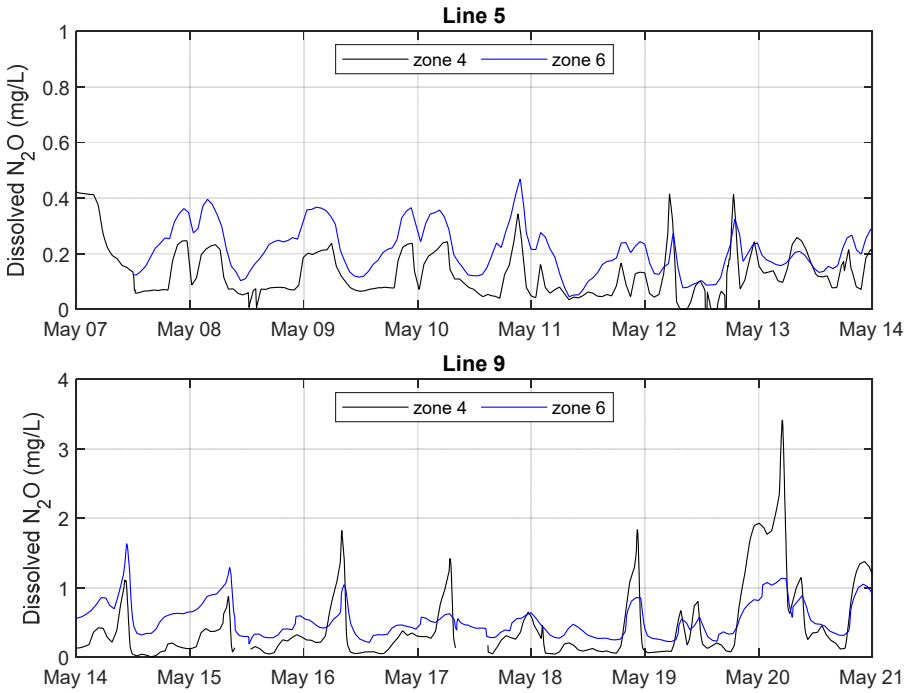

Figure 24. Readings from dissolved N_2O probes in zones 4 and 6 for line 5 (top) and line 9 (bottom). Note the difference in y-axis scale between the two graphs.

Compared to the water quality parameters from this same time period (Figure 21, section 5.3), N_2O concentration peaks seemed to occur shortly after peaks in dissolved NH_4^+. Online dissolved N_2O and combined dissolved NO_2^- and NO_3^- followed a similar trend, but both trends are likely interlinked. Decreases in pH and alkalinity were also observed concurrently with increases in N_2O. This suggests that N_2O production is indeed occurring during nitrification, as has been proposed in previous research at Viikinmäki by Kosonen et al. (2016) and Blomberg et al. (2018). Aeration and DO also seemed to be related to N_2O production and emission, as would be expected since increased aeration results in increased stripping of N_2O. Aeration of additional zones is also controlled by the NH_4^+ concentration, linking N_2O production to nitrification once again. Due to the interconnected nature of all monitored water quality parameters, it is difficult to decipher the exact relationship between N_2O and any single parameter.

The largest consecutive monitoring campaign occurred in zone 4 of line 9, so data from this zone were used to calculate estimated off-gas N_2O concentrations using equation 8 from section 2.2.2. The mass transfer K_La was estimated using three methods. The first method, labeled the superficial velocity method, used Foley et al.'s superficial velocity power law estimation (equation 14, section 2.2.2). In the second method, the static method, a single K_La that minimized the sum of squared errors (SSE) between estimated and measured N_2O values was calculated. The third method, or O_2 method, calculated N_2O K_La based on the O_2 K_La and the diffusion coefficients of N_2O and O_2 (equation 2, section 2.2.1). A fourth possible method for estimating αK_La from steady-state conditions (equation 13, section

2.2.2) was ruled out because the dissolved N_2O was too variable with time to be considered steady-state. In all three methods used, K_La was adjusted for temperature.

Static correction factors were applied in the superficial velocity and O_2 methods in order to reduce the SSE between measured and calculated N_2O values. These factors were solved for using Excel solver evolutionary method with constraints. A correction factor of 2.49 was applied in the superficial velocity method and a correction factor of 0.45 was applied to the O_2 method. Prior to these correction factors, the O_2 method significantly over-estimated N_2O emissions while the superficial velocity method under-estimated N_2O emissions.

Based on SSE, the corrected O_2 method for K_La estimation led to the most accurate calculated N_2O values. The corrected superficial velocity method performed second best and did not overestimate May 20 N_2O production as much as the O_2 method (Figure 25). All three models provided representative estimates once calibrated for the measurement period, but all models under-estimated N_2O production at the start of the week and over-estimated at the end of the week.

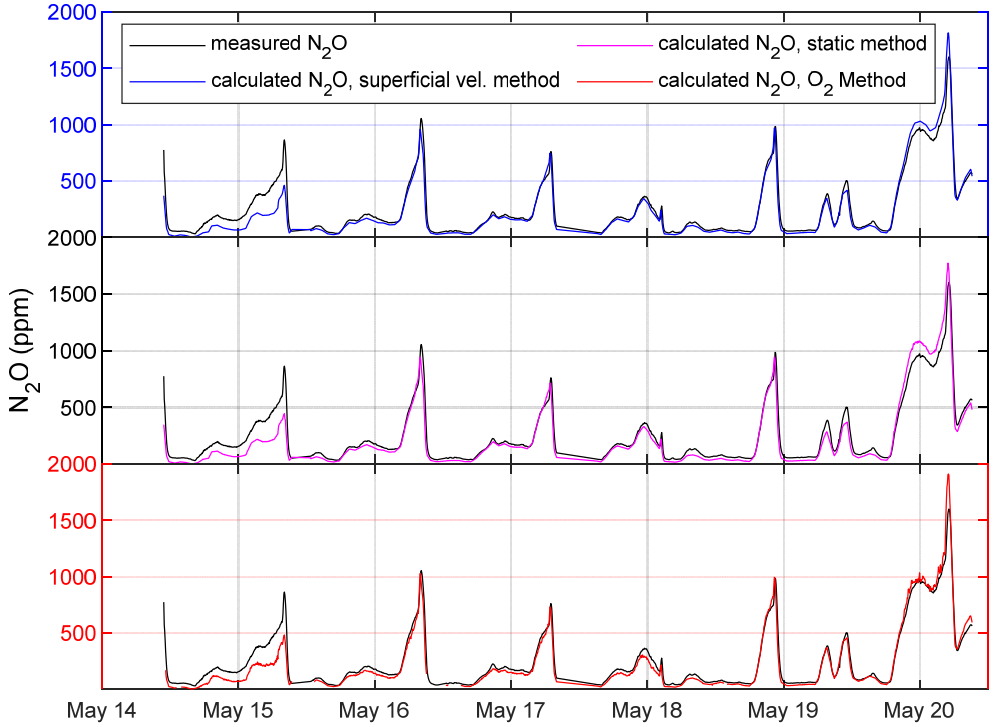

Figure 25. Measured and calculated N_2O concentrations for all three K_La calculation methods.

For the superficial velocity and O_2 methods of K_La calculation, the resulting values were highly influenced by air flowrates. The static method was not affected by flowrates, and the solved static αK_La value of 24.9 d^{-1} was below the average αK_La values of 29.1 and 32.9 d^{-1} for the superficial velocity and O_2 methods, respectively. A comparison of the calculated αK_La values over time is shown in Figure 26.

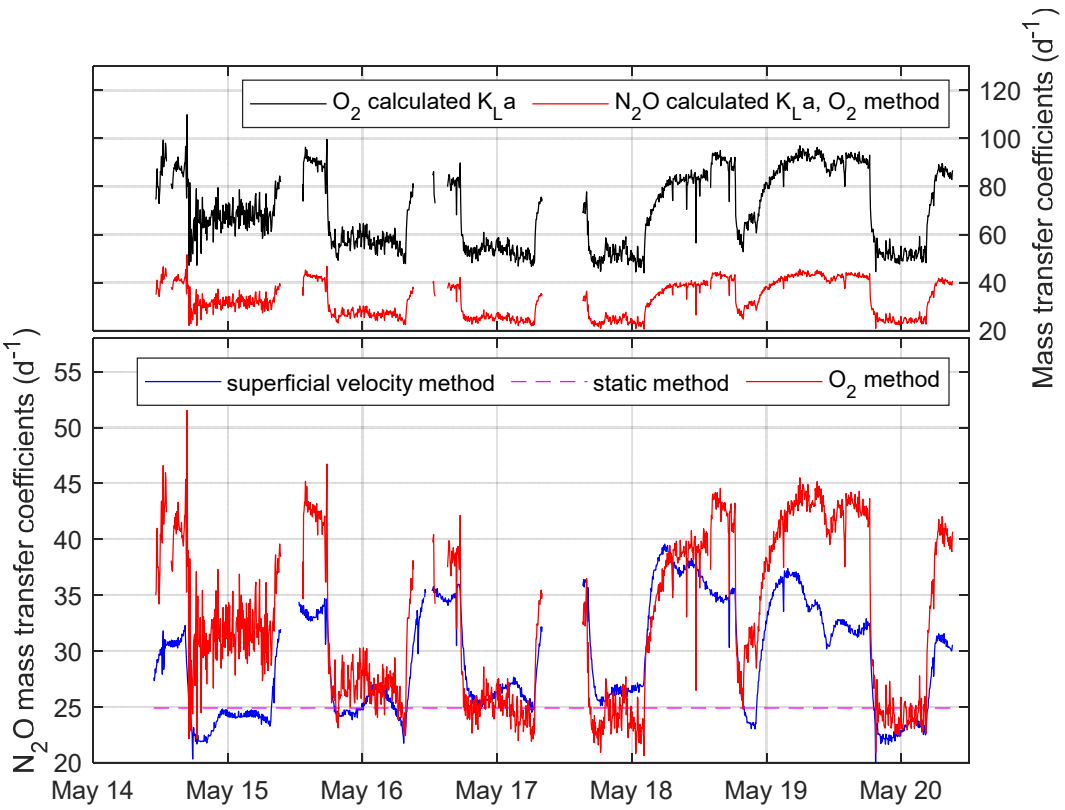

Figure 26. Comparison of mass transfer coefficients for N_2O and O_2 in zone 4 of line 9. Top: O_2 K_La compared against calculated O_2 method N_2O K_La. Bottom: N_2O mass transfer coefficients for superficial velocity, static, and O_2 methods. Superficial velocity and O_2 method N_2O mass transfer coefficients have already had their respective static correction factors applied prior to graphing.

In the O_2 transfer tests, OTE was the highest on the 14th-15th and 19th-20th of May. The alpha correction factor comparing OTE to SOTE would therefore be highest during the start and end of the week. The O_2 K_La method provided the highest accuracy for N_2O estimation, suggesting similarities between the kinetics of O_2 and N_2O transfer. It would therefore be interesting to test if accuracy would increase or decrease if a dynamic alpha factor for O_2 were used in the calculations.

In the current calculations for the O_2 K_La method, the exact value for alpha is unknown and alpha is treated as part of the volumetric mass transfer coefficient when solving for N_2O K_La using equation 2 from section 2.2.1. If the alpha factor was explicitly known it could be divided out and re-applied to the N_2O K_La, potentially with greater accuracy. However, N_2O transfer was higher than modeled values at the start of the week and lower than modeled values at the end of the week. Direct application of O_2 alpha values would likely increase the over-estimation of N_2O emissions at the end of the week and would likely not be sufficient to correct for all differences in modeled and measured N_2O transfer. Other factors such as N_2O production may need to be considered in order to further improve accuracy.

Prior to modification with the static correction factor of 2.49, the superficial velocity method calculated N_2O K_La values between 7.9 and 15.9 d^{-1} that underestimated N_2O emissions. In

comparison, Foley et al.'s study (2010) calculated K_La values ranging from approximately 10 to 90 d^{-1} in activated sludge basins up to 6 m deep. The tanks at Viikinmäki are 12 m deep, so Foley et al.'s empirical relationship may not represent greater depths as accurately. The αK_La values calculated from experimental O_2 values, prior to application of the static correction factor of 0.45, ranged from 46 to 116 d^{-1} at 20 °C and over-estimated N_2O emissions on all days except for the 15th, when all models under-estimated emissions. In an N_2O model by Fiat (2019), N_2O K_La values of over 2600 d^{-1} were estimated for a fixed bed bio-film reactor based off estimated O_2 K_La values of a similar magnitude. It is therefore clear that the selected method for estimating K_La values for N_2O mass transfer, as well as the selected model, can have a significant effect on model results.

5.5 Local and Plant-Wide Emissions

During the measurement campaign, local N_2O emissions were measured from lines 5 and 9. In addition, N_2O measurements from the entire Viikinmäki WWTP were recorded. On average, air flow to each aeration basin makes up under 1 % of the total treatment plant air released from Viikinmäki, for a total contribution from all 9 aeration basins of less than 10 %. Despite the non-negligible contribution of N_2O emissions from the secondary clarifiers (Mikola, et al., 2014), air flow from the secondary clarifiers is significantly less and emissions from Viikinmäki would be expected to primarily reflect emissions from the aeration basins. Full plant emissions should have lower concentrations than activated sludge basin emissions due to dilution, and there is a delay between off-gas release from the basins and off-gas release from the Viikinmäki WWTP.

Figure 27 shows the relationship between the measured local N_2O values and the plant-wide N_2O emissions. At the start of the measurement campaign there is insufficient data to suggest that the emissions from line 5 are representative of trends in the plant as a whole.

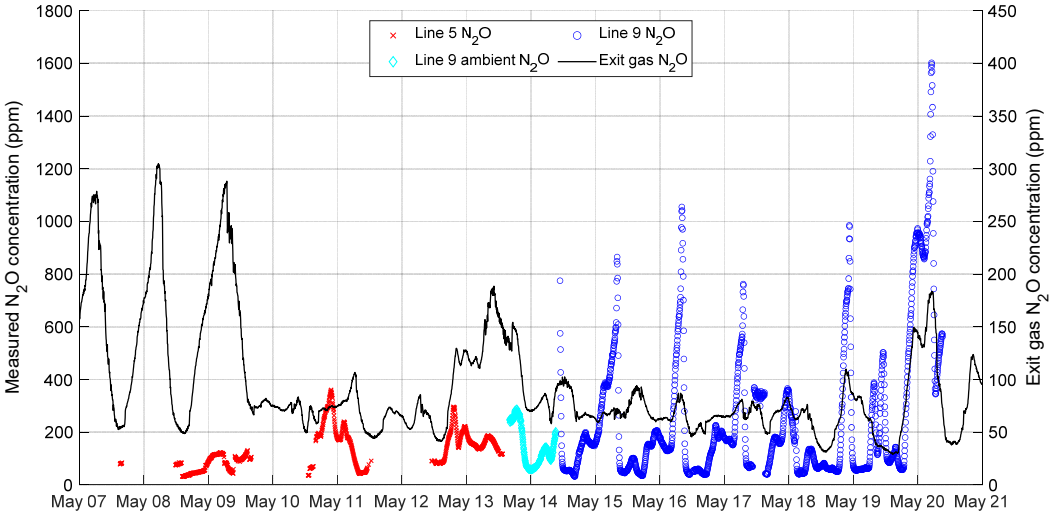

Figure 27. Local and plant-wide N_2O emissions during the measurement campaign.

Line 9 measurements show peaks at similar times to some of the plant-wide peaks, and peaks are often close to 10 % of the concentration from line 9, but it is clear that not all lines have the same N_2O emissions and that some lines may have slightly different temporal variation than line 9 (Figure 28).

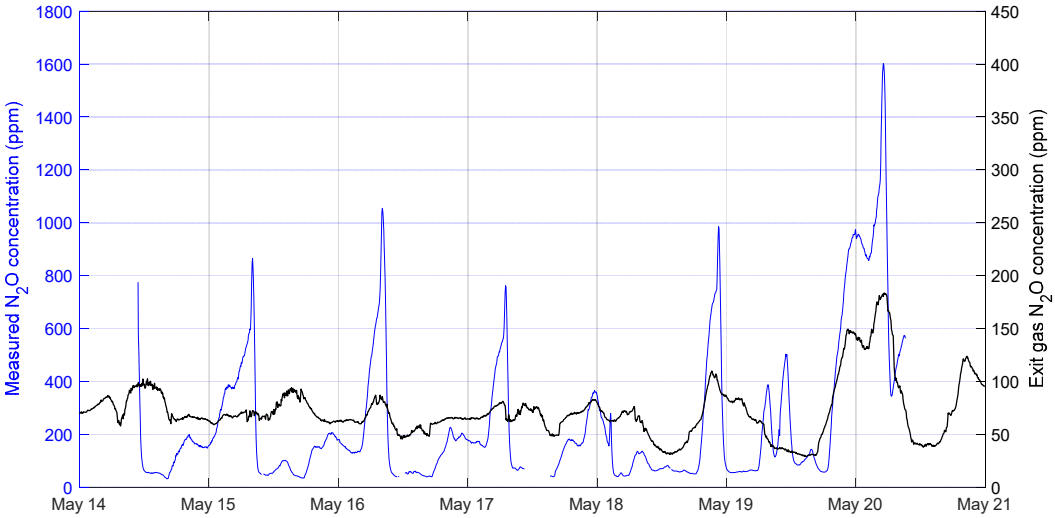

Figure 28. Line 9 zone 4 and plant-wide N_2O emissions during week 2 of the measurement campaign.

This difference between treatment lines makes it difficult to model N_2O emissions based on conditions in a single line, as conditions in each line must be taken into consideration.

5.6 Nitrous Oxide Emission Factor

The N_2O EF was calculated per equation 20 in section 4.3.1, with slight changes based on data availability. Neither influent TN nor influent wastewater flow were recorded within this thesis, even though these values were likely available from Viikinmäki WWTP. Instead, the TN after primary settling and the effluent wastewater flow were substituted. Primary settling typically removes less than 10 % of influent TN, and additional TN enters the primary settling basin via the reject water from sludge digestion. Therefore, the pre-settling TN was assumed to be equivalent to influent TN. No significant accumulation of wastewater occurs within Viikinmäki, so effluent flow is assumed equal to influent flow. The average TN after pre-settling was 53.15 mg/L based on laboratory values from 6-23 May, and the average effluent flowrate from Viikinmäki was 3 m^3/s from 7-20 May. From averages taken from 7-20 May, the exit gas flowrate was approximately 124 m^3/s and N_2O made up just over 92 ppm of the exit gas, or 0.11 mg-N/L at the average conditions of 11 °C and 1.02 bar during this time period.

During this period of unusual conditions, Viikinmäki had an average EF of 8.5 % influent nitrogen released as N_2O. This is greater than the previous highest EF of 2.8 % in June 2013 (Kosonen, et al., 2016). However, it should be noted that the EF for the time period of 7-20 May does not represent the average emissions for 2019 as a whole. The cause for this

significant change in N_2O EFs between studies is likely increased N_2O production within the wastewater rather than variations in N_2O stripping. Dissolved N_2O values from this study were also significantly higher than in the previous study by Blomberg (2016), where maximum recorded dissolved N_2O concentrations were 0.4 mg-N/L. In comparison, dissolved N_2O concentrations over 3.5 mg-N/L were recorded in line 9 during this study.

5.7 Potential Sources of Error

During the time period of data collection, dissolved and emitted N_2O concentrations were significantly elevated compared to average conditions. This could potentially limit the applicability of collected data to normal operations at Viikinmäki, but also suppresses potential "noise" from measurements. The two-week sampling period was too short to gain insight to gas stripping during average conditions at Viikinmäki, even if the plant had not been in upset conditions.

During the vertical profile tests on 1 July, continuous data showed that insufficient time was provided to reach an ambient stabilized reading at each depth. Uncertainty also existed in the exact depth measured, as depth markings were re-made before each test day and the reference 0 m depth appeared to differ by up to half a meter. Between the 5 m and 8 m markings an additional half meter of difference was introduced, likely due to coiling in the line that was being marked for distance, but depths past 5 m were not used for the depth profile. This depth uncertainty does not affect the measured N_2O concentrations and the lack of stable readings likely affected all measurements to a similar degree, so the minimal variation of dissolved N_2O at all depths measured should still hold true. Additional error could be introduced by assuming the bottom 7 m of the Viikinmäki WWTP behaves the same as the top 5 m, and this is considered in the sensitivity analysis in section 5.8 below.

Sources of error within O_2 transfer tests include noise and drift in the O_2 analyzer signal and lag time of sample gas in tubing before being measured. The AMI model 65 is reported to have a repeatability within ± 0.1 % and a drift under 1 % of the full range over 4 weeks (AMI, n.d.). Based on average velocities of off-gas air, samples would take on average 0.1 minutes to travel from the floating hood to the O_2 sampling point and 0.4 minutes to travel from the Alphameter through smaller tubing to the O_2 sampling point. From the sampling point, air was drawn at 0.94 L/min through less than 1 m of 0.3 cm (1/8 inch) diameter tubing to the O_2 analyzer which has a response time of ≤ 13 seconds for an additional lag time of up to 0.25 minutes. Therefore, the average sample should have been collected by the gas hood within 1 minute of the recorded time. Additional sources of uncertainty include temperature variation between the locations of the temperature probe and gas hood, temperature probe integrity, and local variation in aeration air flowrates.

Sources of error within N_2O transfer tests were limited to uncertainties in probe or Gasmet readings, but additional uncertainties were likely introduced to the modeled N_2O emissions though local variations in air flowrates and temperature. Probe noise and signal errors caused

occasional incorrect readings for probes, but clear outliers were removed as outlined in section 4.4. The expected Gasmet DX4015 error is listed in Table 4.

Table 4. Gasmet DX4015 calibration, measurement drift, and deviation (Gasmet, 2018).

Zero-point calibration	Every 24 hours, calibrate with N_2 (5.0 or higher recommended)
Zero-point drift	< 2 % of measuring range per zero-point calibration interval
Sensitivity drift	None
Linearity deviation	< 2 % of measuring range
Temperature drifts	< 2 % of measuring range per 10 K temperature change
Pressure influence	1 % change of measuring value for 1 % sample pressure change. Ambient pressure changes measured and compensated.

5.8 Sensitivity Analysis

Key variables affecting the N_2O and O_2 transfer were analyzed for their impact on the results. Temperature readings up to 1 °C off from the true temperature were found to have minimal effects, while a 10 % difference in air flowrate had a fairly significant impact on O_2 transfer, with peak differences around 15 % higher or lower than initial measured values (Figure 29). Erroneous O_2 off-gas readings with 0.2 % error had a similar level of impact on calculated O_2 transfer variables, and errors in measuring dimensions were also potentially significant (Appendix 3).

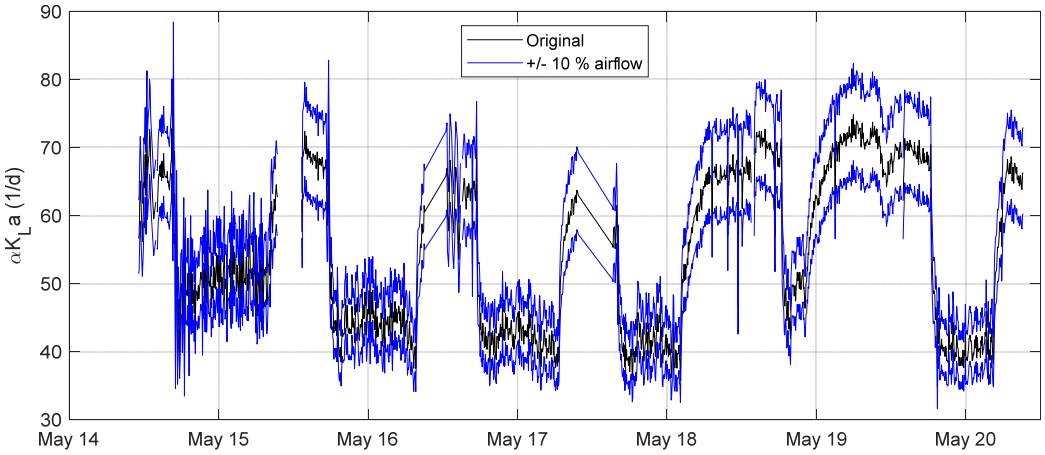

Figure 29. Impact of airflow variation on O_2 transfer $\alpha K_L a$ values compared to original calculated values.

For up to 10 % changes in dissolved N_2O readings, the average variation for a 20 % change across the full basin depth, the calculated off-gas N_2O could change by up to 10 % from initial calculations (Figure 30). However, it should be noted that the dissolved N_2O was still treated as constant with depth for this analysis.

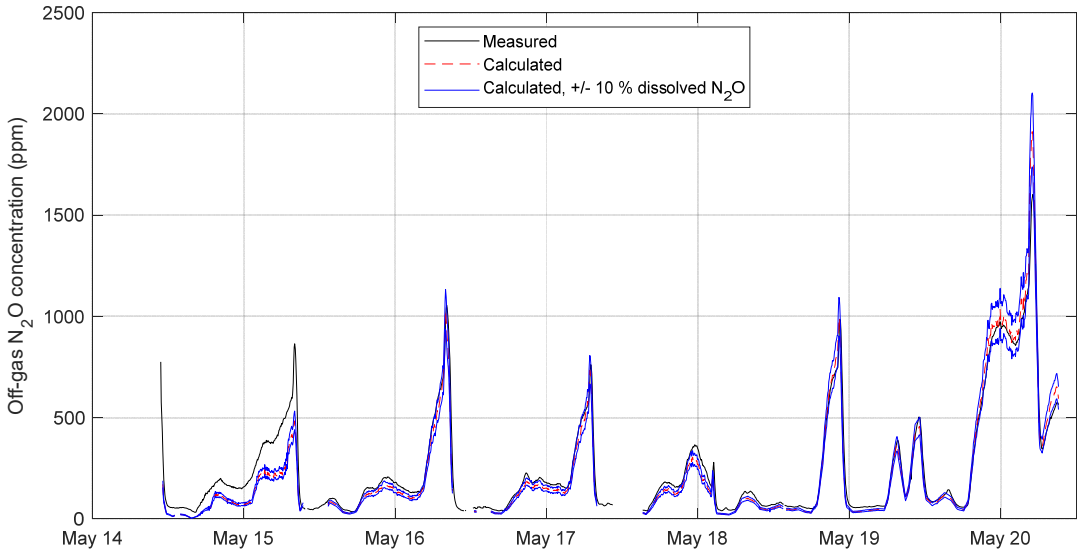

Figure 30. Impact of dissolved N_2O readings on calculated off-gas N_2O using O_2 method. Compared against measured N_2O values.

For N_2O calculations, the choice of mass transfer coefficient (αK_La) had a significant impact on the calculated results, though this was partly due to the high level of variability attached to the αK_La. For a range of +/- 50 %, similar to the variability seen in O_2 αK_La values, calculated N_2O values changed by +/- 25 % compared to initial calculations (Figure 31).

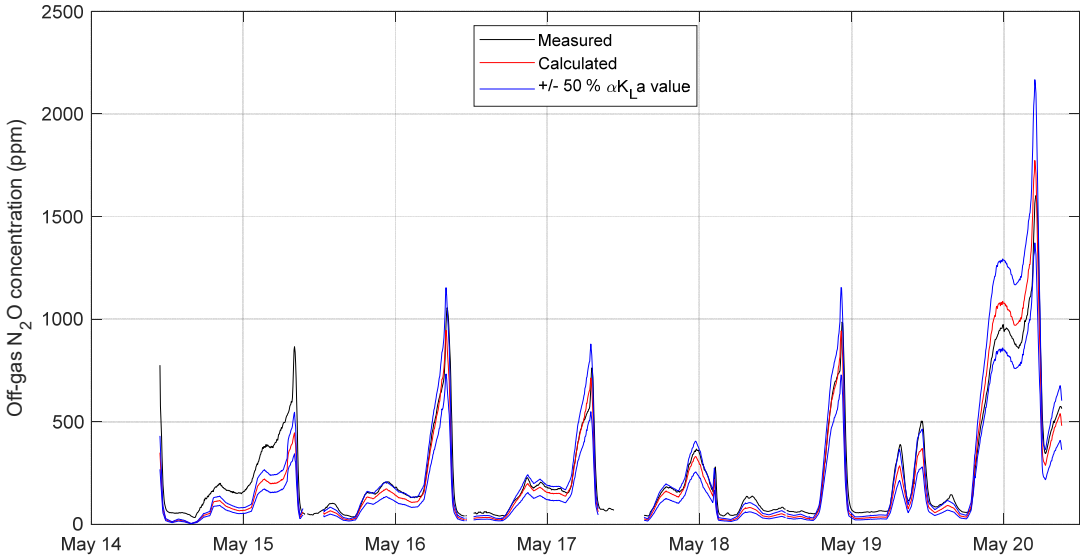

Figure 31. Impact of changing mass transfer coefficient on calculated off-gas N_2O using static method. Compared against measured N_2O values.

Incorrect zone dimensions also have an impact on the calculated mass transfer coefficients for O_2 and N_2O, but the resulting error should be reduced by continuous use of the same incorrect dimensions in off-gas calculations. From the sensitivity analysis, it can be inferred that the assumptions made and the accuracy of data collected are important to model accuracy. However, it was also evident that small errors did not undermine the overall model integrity. Graphical data from additional sensitivity analyses are available in Appendix 3.

5.9 Modeling Implications

Accurate modeling of N_2O emissions would allow for selection of operational strategies that reduce N_2O emissions for wastewater treatment. An accurate N_2O emissions model based on dissolved N_2O concentrations would also enable estimation of N_2O emissions in situations where off-gas measuring is more difficult, such as from uncovered basins. The basic N_2O stripping model used in this thesis is applicable in many different processes, but significant limitations still exist to modeling N_2O emissions from dissolved N_2O.

The selected K_La for modeling N_2O stripping has a significant impact on the estimated N_2O emissions, as can be seen in sections 5.6 and 5.8. Accurate determination of the local mass transfer coefficient is therefore essential to a successful N_2O modeling campaign. The dynamic nature of mass transfer with aeration and water quality conditions results in inherent error from the use of a single representative K_La, but the use of a dynamic K_La or dynamic correction factor requires a more complicated model.

Within this study, changes to the K_La value did not seem to explain all variations between measured and modeled N_2O. Dissolved N_2O values had a significant impact on estimated off-gas, so selection of a representative location for N_2O measurements is also necessary in order to model off-gas for an entire basin as opposed to for a single location within the basin. Modeling emissions for an entire plant with multiple treatment lines may not be realistic, as Viikinmäki's varying conditions between lines 5 and 9 reinforce that no two treatment lines behave exactly the same.

Additional research is needed to clarify the best practices for K_La and alpha correction estimation in N_2O stripping models. Estimation of N_2O αK_La based on measured O_2 αK_La requires a better understanding of the impact of water quality on diffusivity and transfer rate for both N_2O and O_2.

6 Conclusions and Future Work

In this thesis, N_2O and O_2 transfer were simultaneously studied from a full-scale activated sludge basin for the first time. The measurement array used for continuous measurement was very effective but could be further improved on if used in future studies.

Despite issues encountered during depth profile measurements, no obvious vertical N_2O stratification was measured in this study. This allows for simplifying assumptions to be used when estimating N_2O mass transfer. Dissolved N_2O probes were reinforced as a reliable way to observe changes in N_2O production and emission, although estimating an accurate off-gas concentration from dissolved concentrations requires a better understanding of the mass transfer kinetics. Additionally, complications can arise when estimating emissions in plants with multiple treatment lines. Unless all lines perform similarly, it is difficult to estimate the full plant's emissions based on conditions in one line.

Transfer of O_2 depended most heavily on aeration air flowrates, with variations from this trend assumed to be caused by unknown water quality conditions. Emissions of N_2O depended most heavily on dissolved N_2O concentrations but were also impacted by air flowrates and water quality. Mass transfer K_La values for N_2O calculated based on diffusivities and O_2 K_La values were found to model N_2O emission slightly better than K_La values based on superficial velocity or a static K_La of best fit. Although it was difficult to find comparative K_La values, calculated O_2 and N_2O K_La values were within a similar range of values used in other studies. Transfer of O_2 and N_2O changed with similar magnitude based on aeration flowrates, but the variation in diffusivity between N_2O and O_2 was different than in literature values for clean water. This is likely because the degree to which N_2O and O_2 diffusivities are impacted by water quality is not the same, but further research would be necessary to confirm this.

Sensitivity analyses confirmed that dissolved N_2O and selected K_La values have a significant effect on modeled N_2O emissions. For modeling purposes, representative locations must be selected for dissolved N_2O measurements. The choice of K_La and correction factors should also be carefully considered and, if possible, mass transfer coefficients should be determined experimentally for the location and conditions that are going to be modeled.

The attempted depth profile was not satisfactorily completed in this study, so additional depth studies could improve knowledge of changes in wastewater conditions in deep aeration basins. This study consisted of measurements from a very short period of a time. A longer study period could increase certainty in findings and conclusions, but care should be taken to narrow the focus of future studies as the scope of this study was slightly too broad for in-depth analysis of all collected data.

The results from this study can hopefully be used alongside the existing N_2O model at Viikinmäki to improve modeling of N_2O emissions from biological N_2O production in the

activated sludge basins. Further research is recommended on the impacts of water quality conditions on N_2O transfer in order to more accurately correct mass transfer under changing conditions. Additional studies on conditions leading to N_2O production within Viikinmäki and variations between lines would continue to improve this model.

References

Ahn, J. H. et al., 2010. Spatial and Temporal Variability in Atmospheric Nitrous Oxide Generation and Emission from Full-Scale Biological Nitrogen Removal and Non-BNR Processes. *Water Environment Research,* December, 82(12), pp. 2362-2372.

Ahn, J. h. et al., 2010. N2O Emissions from Activated Sludge Processes, 2008-2009: Results of a National Monitoring Survey in the United States. *Environmental Science & Technology,* May, 44(12), pp. 4505-4511.

AMI, n.d. *MODEL 65.* [Online] Available at: https://www.amio2.com/products/details/Model-65/ [Accessed September 2019].

ASCE, 2007. *Measurement of oxygen transfer in clean water. ASCE standard.,* Reston, Virginia: American Society of Civil Engineers.

Bandyopadhyay, B. & Humphrey, A. E., 1967. Dynamic Measurement of the Volumetric Oxygen Transfer Coefficient in Fermentation Systems. *Biotechnology and Bioengineering,* Volume IX, pp. 533-544.

Baresel, C., Andersson, S., Yang, J. & Andersen, M. H., 2016. Comparison of nitrous oxide (N2O) emissions calculations at a Swedish wastewater treatment plant based on water concentrations versus off-gas concentrations. *Advances in Climate Change Research,* 7(3), pp. 185-191.

Bellandi, G. et al., 2018. Multi-point monitoring of nitrous oxide emissions in three full-scale conventional activated sludge tanks in Europe. *Water Science & Technology,* 77(4), pp. 880-890.

Blomberg, K., 2016. *Modelling nitrous oxide production and emissions at a wastewater treatment plant,* Espoo, Finland: s.n.

Blomberg, K. et al., 2018. Development of an Extended ASM3 Model for Predicting the Nitrous Oxide Emissions in a Full-Scale Wastewater Treatment Plant. *Environmental Science and Technology,* May, 52(10), pp. 5803-5811.

Caivano, M. et al., 2017. Disinfection Unit of Water Resource Recovery Facilities: Critical Issue for N2O Emission. In: G. Mannina, ed. *Frontiers in Wastewater Treatment and Modelling: FICWTM 2017.* s.l.:s.n., pp. 444-450.

Chandran, K., 2011. Protocol for the measurement of nitrous oxide fluxes from biological wastewater treatment plants. In: M. G. Klotz, ed. *Methods in Enzymology.* s.l.:s.n., pp. 369-385.

Czepiel, P., Crill, P. & Harriss, R., 1995. Nitrous Oxide Emissions from Municipal Wastewater Treatment. *Environmental Science & Technology,* 1 September, 29(9), pp. 2352-2356.

Daelman, M. et al., 2015. Seasonal and diurnal variability of N2O emissions from a full-scale municipal wastewater treatment plant.. *Science of the Total Environment,* December, Volume 536, pp. 1-11.

De Temmerman, L. et al., 2015. The effect of fine bubble aeration intensity on membrane bioreactor sludge characteristics and fouling. *Water Research,* June, Volume 76, pp. 99-109.

Duan, H. et al., 2017. Quantifying nitrous oxide production pathways in wastewater treatment systems using isotope technology – A critical review. *Water Research,* Volume 122, pp. 96-113.

Emami, N., Sobhani, R. & Rosso, D., 2018. Diurnal variations of the energy intensity and associated greenhouse gas emissions for activated sludge processes. *Water Science & Technology,* 77(7), pp. 1838-1850.

EPA, 1989. *Design Manual: Fine Pore Aeration Systems,* Washington DC, USA: U.S. Environmental Protection Agency.

EPA, 1999. *Wastewater Technology Factsheet: Fine Bubble Aeration,* Washington D.C., USA: U.S. Environmental Protection Agency.

EPA, 2016. *Global Mitigation of Non-CO2 Greenhouse Gases: Wastewater.* [Online] Available at: https://www.epa.gov/global-mitigation-non-co2-greenhouse-gases/global-mitigation-non-co2-greenhouse-gases-wastewater [Accessed July 2019].

EPA, 2019. *Inventory of U.S. Greenhouse Gas Emissions and Sinks: 1990-2017,* s.l.: s.n.

EU Parliament, 2006. Regulation (EC) No 166/2006 of the European Parliament and of the Council of 18 January 2006 concerning the establishment of a European Pollutant Release and Transfer Register and amending Council Directives 91/689/EEC and 96/61/EC. *Official Journal of the European Union,* 18 January.

Fiat, J., 2019. *Analyse et modélisation des émissions de protoxyde d'azote par les biofiltres nitrifiants tertiaires à échelle industrielle,* Toulouse, France: s.n.

Foley, J., de Haas, D., Yuan, Z. & Lant, P., 2010. Nitrous oxide generation in full-scale biological nutrient removal wastewater treatment plants. *Water Research,* 44(3), pp. 831-844.

Fred, T., n.d. *Efficient purification of waste waters.* [Online] Available at: http://www.itamerihaaste.net/en/frontpage_(vanha)/bank_of_actions/efficient_purification_of_waste_waters.581.xhtml [Accessed September 2019].

Gasmet, 2018. *DX4015 FTIR Gas Analyzer.* [Online] Available at: https://www.gasmet.com/wp-content/uploads/2018/03/Gasmet-DX4015-Technical-Data-ID-7090.pdf [Accessed September 2019].

Gasser, T. et al., 2017. Accounting for the climate–carbon feedback in emission metrics. *Earth System Dynamics,* Volume 8, pp. 235-253.

Haimi, H., 2016. *Data-derived soft sensors in biological wastewater treatment with application of multivariate statistical methods,* Espoo, Finland: s.n.

Hall, K. C., 1980. Gas Chromatographic Measurement of Nitrous Oxide Dissolved in Water Using a Headspace Analysis Technique. *Journal of Chromatographic Science,* 18(1), pp. 22-24.

Hanaki, K., Hong, Z. & Matsuo, T., 1992. Production of Nitrous Oxide Gas During Denitrification of Wastewater. *Water Science Technology,* 26(5-6), pp. 1027-1036.

Higbie, R., 1935. The rate of absortion of a pure gas into a still liquid during short periods of exposure. *Transactions of the American Institute of Chemical Engineers,* Volume 31, pp. 365-388.

HSY, 2015. *Viikinmäki wastewater treatment plant.* [Online] Available at: https://www.hsy.fi/en/experts/water-services/wastewater-treatment-plants/viikinmaki/Pages/default.aspx [Accessed June 2019].

HSY, 2016. *Helsinki Metropolitan Area Climate Strategy.* [Online] Available at: https://www.hsy.fi/en/experts/climatechange/mitigation/Pages/mitigation_strategy_and_targets.aspx [Accessed September 2019].

HSY, 2018. *Jätevedenpuhdistus pääkaupunkiseudulla 2017: Viikinmäen ja Suomenojan puhdistamot,* Helsinki, Finland: s.n.

HSY, 2019. *Ilmastus (DN-prosessi).* Helsinki, Finland: s.n.

Hu, J., 2006. *Evaluation of Parameters Influencing Oxygen Transfer Efficiency in a Membrane Bioreactor,* Honolulu, HI: s.n.

IPCC, 2006. Wastewater Treatment and Discharge. In: *2006 IPCC Guidelines for National Greenhouse Gas Inventories Volume 5: Waste.* s.l.:s.n.

IPCC, 2013. *Climate Change 2013: The Physical Science Basis.,* Cambridge, U.K. and New York, NY, USA: Cambridge University Press.

IPCC, 2019. In: *2019 Refinement to the 2006 IPCC Guidelines for National Greenhouse Gas Inventories.* s.l.:s.n.

Jiang, L.-M.et al., 2017. Modelling oxygen transfer using dynamic alpha factors. *Water Research,* Volume 124, pp. 139-148.

Kampschreur, M. J. et al., 2007. Unraveling the Source of Nitric Oxide Emission During Nitrification. *Water Environment Research,* December, 79(13), pp. 2499-2509.

Kampschreur, M. J. et al., 2009. Nitrous oxide emission during wastewater treatment. *Water Research,* September, 43(17), pp. 4093-4103.

Kampschreur, M. J. et al., 2008. Dynamics of nitric oxide and nitrous oxide emission during full-scale reject water treatment. *Water Research,* February, 42(3), pp. 812-826.

Kosonen, H., 2013. *Nitrous oxide emissions at the Viikinmäki wastewater treatment plant - results and process correlations found in a long-term on-line monitoring campaign,* Espoo, Finland: s.n.

Kosonen, H. et al., 2016. Nitrous Oxide Production at a Fully Covered Wastewater Treatment Plant: Results of a Long-Term Online Monitoring Campaign. *Environmental Science & Technology,* 7 June, 50(11), pp. 5547-5554.

Kosse, P., Lübken, M., Schmidt, T. C. & Wichern, M., 2017. Quantification of nitrous oxide in wastewater based on salt-induced stripping. *Science of the Total Environment,* December, Volume 601-602, pp. 83-88.

Kozlowski, J. A., Price, J. & Stein, L. Y., 2014. Revision of N2O-Producing Pathways in the Ammonia-Oxidizing Bacterium Nitrosomonas europaea ATCC 19718. *Applied and Environmental Microbiology,* July, 80(16), pp. 4930-4935.

Law, Y., Ye, L., Pan, Y. & Yuan, Z., 2012. Nitrous oxide emissions from wastewater treatment processes. *Phil. Trans. R. Soc. B,* 5 May, 367(1593), pp. 1265-1277.

Leppänen, M., 2012. *Prosessiolosuhteiden vaikutus jätevedenpuhdistamoiden N2O-päästöihin,* Espoo, Finland: s.n.

Lewis, W. & Whitman, W., 1924. Principles of Gas Transfer Absorption. *Industrial and Engineering Chemistry,* December, 16(12), pp. 1215-1237.

Lizarralde, I. et al., 2018. Validation of a multi-phase plant-wide model for the description of the aeration process in a WWTP. *Water Research,* February, Volume 129, pp. 305-318.

Maja, M., 2018. Wastewater treatment plant monitors its greenhouse gas emissions. *Environmental Science & Engineering Magazine*, 27 June.

Mampaey, K. E., van Dongen, U. G., van Loosdrecht, M. C. & Volcke, E. I., 2015. Novel method for online monitoring of dissolved N2O concentrations through a gas stripping device. *Environmental Technology,* 36(13), pp. 1680-1690.

Matter-Müller, C., Gujer, W. & Giger, W., 1981. Transfer of volatile substances from water to the atmosphere. *Water Research,* 15(11), pp. 1271-1279.

Metcalf & Eddy, I., 2011. *Wastewater Engineering Treatment and Reuse.* Fourth ed. Boston: McGraw-Hill.

Mikola, A. et al., 2014. N2O emissions from secondary clarifiers and their contribution to the total emissions of the WWTP. *Water Science Technology,* 70(4), pp. 720-728.

Moutafchieva, D., Popova, D., Dimitrova, M. & Tchaoushev, S., 2013. Experimental determination of the volumetric mass transfer coefficient. *Journal of Chemical Technology and Metallurgy,* 48(4), pp. 351-356.

NIST, 2018. *NIST Chemistry WebBook, SRD 69: Nitrous Oxide.* [Online] Available at: https://webbook.nist.gov/cgi/cbook.cgi?ID=C10024972&Mask=10 [Accessed July 2019].

NOAA, 2009. *NOAA Study Shows Nitrous Oxide Now Top Ozone-Depleting Emission.* [Online] Available at: https://www.esrl.noaa.gov/news/2009/nitrous_oxide_top_ozone_depleting_gas.html [Accessed July 2019].

NOAA, 2019. *HATS Global N2O.* [Online] Available at: ftp://ftp.cmdl.noaa.gov/hats/n2o/combined/HATS_global_N2O.txt [Accessed June 2019].

Oikeusministeriö, 2008. *Vesioikeuden jätevesienlaskulupa 587/2011 (update to Water Act: license to conduct wastewaters by Water Court 264/1961, Finnish).* s.l.:Suomen Oikeusministeriö.

Painmanakul, P. et al., 2005. Effect of surfactants on liquid-side mass transfer coefficients. *Chemical Engineering Science,* November, 60(22), pp. 6480-6491.

Pascale, R. et al., 2017. Validation of an analytical method for simultaneous high-precision measurements of greenhouse gas emissions from wastewater treatment plants using a gas chromatography-barrier discharge detector system. *Journal of Chromatography A,* January, Volume 1480, pp. 62-69.

Rosso, D., ed., 2018. *Aeration, Mixing, and Energy: Bubbles and Sparks.* s.l.:IWA Publishing.

Rosso, D. & Stenstrom, M. K., 2006. Surfactant effects on a-factors in aeration systems. *Water Research,* 40(7), p. 1397– 1404.

Sander, R., 2015. Compilation of Henry's law constants (version 4.0) for water as solvent. *Atmospheric Chemistry and Physics,* 15(8), pp. 4399-4981.

Schneider, A. G., Townsend-Small, A. & Rosso, D., 2015. Impact of direct greenhouse gas emissions on the carbon footprint of water reclamation processes employing nitrification-denitrification. *Science of the Total Environment,* Volume 505, pp. 1166-1173.

Smith, F. L. & Harvey, A. H., 2007. Avoid Common Pitfalls When Using Henry's Law. *Chemical Engineering Progress (CEP),* September.pp. 33-39.

Tallec, G., Garnier, J., Billen, G. & Gousailles, M., 2006. Nitrous oxide emissions from secondary activated sludge in nitrifying conditions of urban wastewater treatment plants: Effect of oxygenation level. *Water Research,* 40(15), pp. 2972-2980.

Thomson, A. J. et al., 2012. Biological sources and sinks of nitrous oxide and strategies to mitigate emissions. *Philosophical Transactions of the Royal Society B,* May, 367(1593), pp. 1157-1168.

Townsend-Small, A. et al., 2011. Nitrous Oxide Emissions from Wastewater Treatment and Water Reclamation Plants in Southern California. *Journal of Environmental Quality,* 40(5), pp. 1542-1550.

Unisense, n.d. *N2O Wastewater System.* [Online] Available at: https://www.unisense-environment.com/N2O%20Wastewater%20System/ [Accessed February 2019].

Vasilaki, V. et al., 2019. A decade of nitrous oxide (N2O) monitroing in full-scale wastewater treatment processes: A critical review. *Water Research,* 15 September, Volume 162, pp. 392-412.

Vasilaki, V. et al., 2018. Relating N2O emissions during biological nitrogen removal with operating conditions using multivariate statistical techniques. *Water Research,* Volume 140, pp. 387-402.

von Schulthess, R., Kuhni, M. & Gujer, W., 1995. Release of nitric and nitrous oxides from denitrifying activated sludge. *Water Research,* 29(1), pp. 215-226.

WEF, 2009. *Energy Conservation in Water and Wastewater Facilities - MOP 32 (WEF Manual of Practice).* Alexandria: WEF (Water Environment Federation) press; McGraw-Hill Professional.

WEF, 2017. *Liquid Stream Fundamentals: Aeration Design, Fact Sheet.* [Online] Available at: https://www.wef.org/globalassets/assets-wef/direct-download-library/public/03---resources/wsec-2017-fs-024-mrrdc-lsf-aeration-design_final.pdf [Accessed November 2019].

Wunderlin, P. et al., 2012. Mechanisms of N2O production in biological wastewater treatment under nitrifying and denitrifying conditions. *Water Research,* 15 March, 46(4), pp. 1027-1037.

Yu, R., Kampschreur, M. J., van Loosdrecht, M. C. M. & Chandran, K., 2010. Mechanisms and Specific Directionality of Autotrophic Nitrous Oxide and Nitric Oxide Generation During Transient Anoxia. *Environmental Science & Technology,* 44(4), pp. 1313-1319.

Zheng, H., Hanaki, K. & T., M., 1994. Production of Nitrous Oxide Gas During Nitrification of Wastewater. *Water Science Technology,* 30(6), pp. 133-141.

List of Appendices

Appendix 1. Vertical Profile of pH

Table A1. pH and depth measurements from vertical profiles on 2 April and 1 July.

Date	Line; Zone	Depth[1]	pH
2 April	5; 1	0 m	6.65
		4 m	7.05
		6 m	6.75
		8 m	6.7
	5; 6	0 m	6.3
		4 m	6.5
		6 m	6.35
		8 m	6.35
	9; 1	0 m	7.05
		4 m	7.3
		6 m	7.0
		8 m	6.9
	9; 6	0 m	6.6
		4 m	6.6
		6 m	6.5
		8 m	6.45
1 July	9; 6	1 m	6.41
		3 m	6.41
		5 m	6.40

Notes: 1. Combined errors in depth marking accuracy and low visibility of depth markings led to an uncertainty of approximately ± 0.5 m up to 5 m depth and ± 1 m between 5 and 8 m depth.

Appendix 2. Oxygen Transfer Calculations

Table B1. Important constants

Pressure (bar)	1.020	CO2 (%)	0	Elevation (m)	20	(bar)	1.011	Beta (estimated)	0.99

Table B2. Recorded values and measurements (1/3), shared values.

Day	Time	Distance	Position	Reference	Off-Gas	O2 Mole Fraction	O2 Mole Ratio	OTE	αSOTE	T off-gas
		m		mV	mV			(%)	(%)	(°C)
7-May	15:05-15:35	22	5A	210	162	0.162	0.193	27.19	34.77	16.1
8-May	11:40-12:10	30	5C	210	159	0.158	0.188	29.13	35.78	16.2
8-May	12:35-13:00	26	5B	210	159	0.159	0.189	28.73	35.72	16.2
8-May	13:20-13:55	22	5A	210	165	0.164	0.196	25.92	31.83	16.4
9-May	10:30-11:05	48	6A	210	159	0.159	0.189	28.83	34.28	16.9
9-May	15:30-16:00	34	5D	210	154	0.154	0.182	31.31	36.88	16.8
10-May	13:05-13:25	19	4/5baffle	210	186	0.186	0.228	13.84	17.34	16.6
10-May	13:40-14:05	23	5A	209	171	0.171	0.206	22.09	28.41	16.6
13-May	12:30-13:25	47	6A	210	154	0.154	0.182	31.38	36.99	16.9
14-May	11:20-13:55	10	4A	209	182	0.183	0.223	15.70	19.52	15.8
16-May	12.30-14:20	10	4A	210	186	0.186	0.228	14.05	17.54	16.3
16-May	12:40-14:50	10	4α	210	189	0.189	0.232	12.35	15.48	16.4

Table B3. Recorded values and measurements (2/3), gas hood values.

Day	Position	Tww 1	DO 1	Tww 1	C* inf Tww 1	Air vel duct	Air flowrate hood	Air Flux hood	OUR hood	OTR hood	αSOTR hood	αKla hood
		(°C)	mg/L	(deg K)	mg/L	ft/min	m3/h	m3/h/m2	mg/L/h	kgO2/hr	kgO2/hr	1/d
7-May	5A	**15.6**	**2.95**	288.6	14.45	432.5	6.5	8.12	46.92	0.45	0.6	97.94
8-May	5C	16.0	2.48	289.0	14.33	437.5	6.6	8.21	50.85	0.49	0.6	102.99
8-May	5B	15.6	2.63	288.6	14.45	465.0	7.0	8.73	53.31	0.52	0.6	108.21
8-May	5A	15.8	2.48	288.8	14.40	512.5	7.8	9.62	53.00	0.51	0.6	106.66
9-May	6A	16.0	2.09	289.0	14.33	202.5	3.1	3.80	23.30	0.23	0.3	45.69
9-May	5D	15.6	1.98	288.6	14.45	425.0	6.4	7.97	53.10	0.51	0.6	102.17
10-May	4/5baffle	**16.0**	**2.70**	289.0	14.33	610.0	9.2	11.45	33.69	0.33	0.4	69.56
10-May	5A	**16.0**	**3.00**	289.0	14.33	510.0	7.7	9.57	44.96	0.44	0.6	95.27
13-May	6A	15.7	1.99	288.7	14.42	226.3	3.4	4.25	28.32	0.27	0.3	54.69
14-May	4A	15.1	2.64	288.1	14.62	550.0	8.3	10.32	34.46	0.33	0.4	69.05
16-May	4A	15.3	2.68	288.3	14.56	563.3	8.5	10.57	31.59	0.31	0.4	63.85
16-May	4α	15.2	2.73	288.2	14.56	159.8	2.4	3.00	7.88	0.08	0.1	15.98

Notes: Tww refers to temperature readings from DO probes in the wastewater. Bold values taken from plant readings.

Table B4. Recorded values and measurements (3/3), zone values.

Day	Position	T_plant	DO plant	T_plant	C* inf T_plant	AFR zone	Air Flux zone	OUR zone	OTR zone	αSOTR zone	αKla zone
		(°C)	mg/L	(deg K)	mg/L	m3/h	m3/h/m2	mg/L/h	kgO2/hr	kgO2/hr	1/d
7-May	5A	15.56	2.96	288.6	14.46	1186	7.57	43.77	82.29	105.3	91.37
8-May	5C	15.95	2.99	288.9	14.34	1188	7.58	46.97	88.31	113.4	99.27
8-May	5B	15.74	3.01	288.7	14.40	1182	7.54	46.09	86.66	111.4	97.06
8-May	5A	15.80	2.99	288.8	14.39	1193	7.61	41.97	78.91	101.3	88.33
9-May	6A	15.82	2.96	288.8	14.38	513	3.27	20.07	37.74	48.3	42.19
9-May	5D	15.59	2.99	288.6	14.45	1110	7.08	47.17	88.69	113.9	98.81
10-May	4/5baffle	15.98	2.66	289.0	14.33	1639	10.46	30.79	57.90	72.2	63.31
10-May	5A	15.93	2.98	288.9	14.35	1391	8.88	41.71	78.42	100.6	88.05
13-May	6A	15.49	3.00	288.5	14.48	557	3.55	23.72	44.59	57.2	49.56
14-May	4A	15.62	2.83	288.6	14.44	1370	8.74	29.20	54.89	69.5	60.33
16-May	4A	15.98	3.08	289.0	14.33	1636	10.44	31.20	58.67	76.0	66.56
16-May	4α	15.96	3.09	289.0	14.34	1636	10.44	27.43	51.57	66.9	58.53

Appendix 3. Sensitivity Analysis Graphs

A3.1 Continuous Oxygen Transfer Tests

For continuous O_2 transfer tests, sensitivity analysis was performed for the effects of airflow, O_2 and DO readings, dimensions, and temperature on OTR, $\alpha K_L a$, and OTE. Temperature and DO readings appeared to affect the resulting calculations the least, while the impacts of variations in off-gas O_2 readings, airflow, and dimensions were more significant.

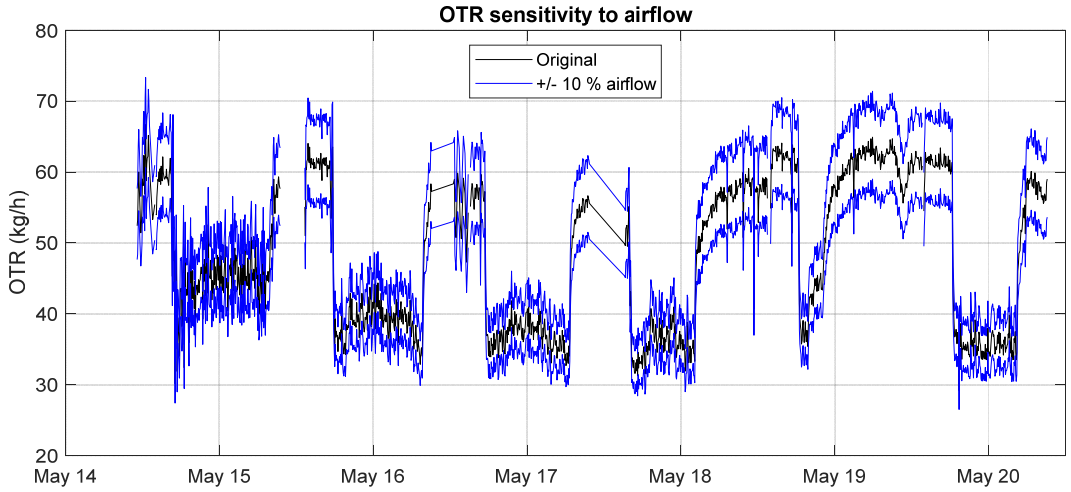

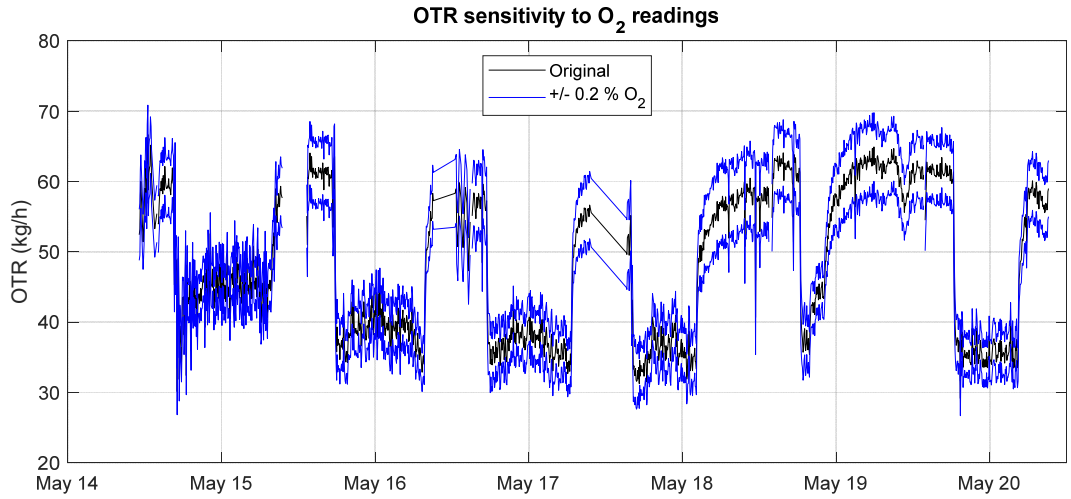

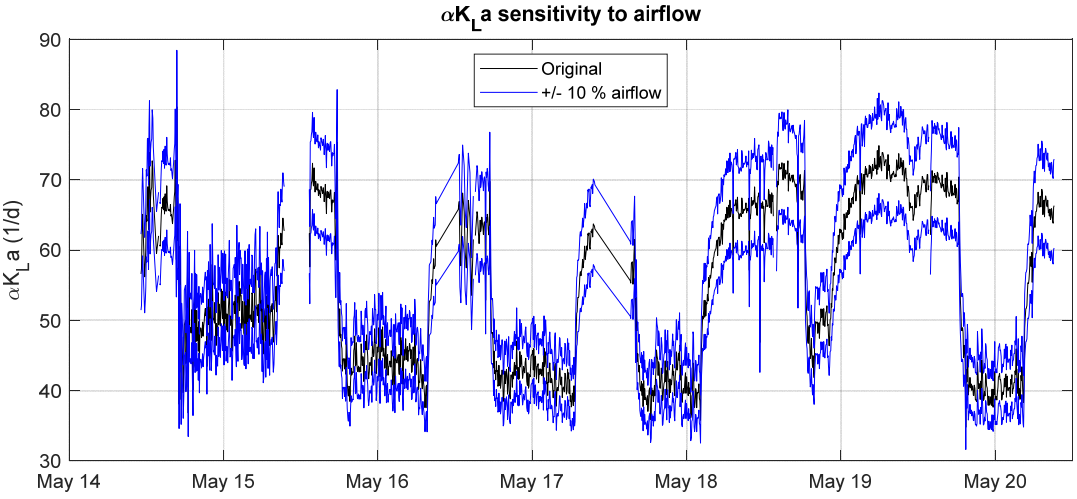
αK_L a sensitivity to airflow
Original
+/- 10 % airflow
αK_L a (1/d)
90
80
70
60
50
40
30
May 14
May 15
May 16
May 17
May 18
May 19
May 20

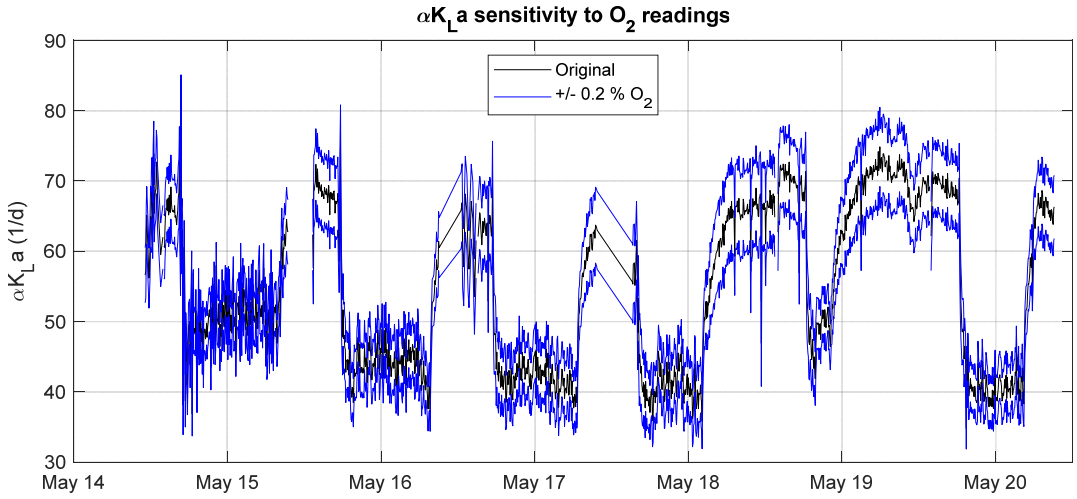
αK_L a sensitivity to O_2 readings
Original
+/- 0.2 % O_2
αK_L a (1/d)
90
80
70
60
50
40
30
May 14
May 15
May 16
May 17
May 18
May 19
May 20

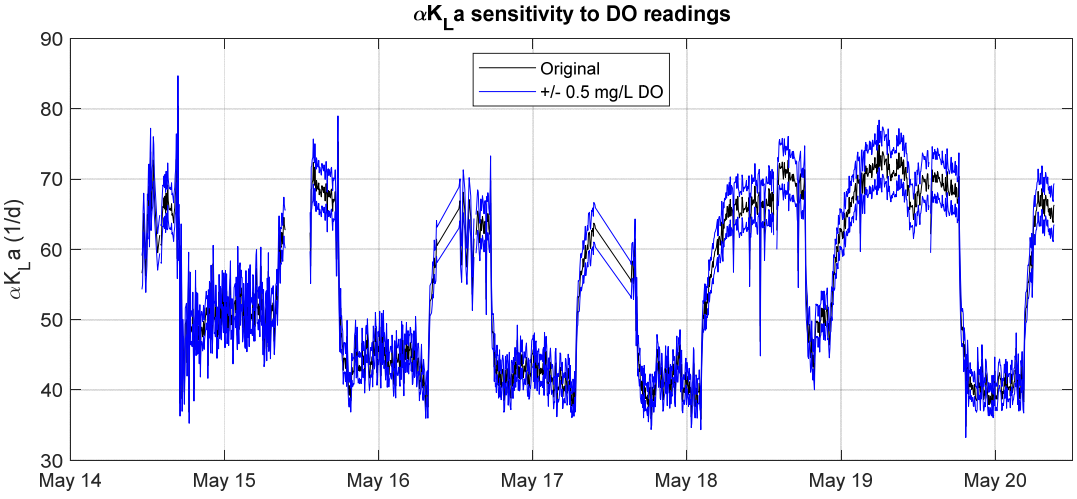
αK_L a sensitivity to DO readings
Original
+/- 0.5 mg/L DO
αK_L a (1/d)
90
80
70
60
50
40
30
May 14
May 15
May 16
May 17
May 18
May 19
May 20

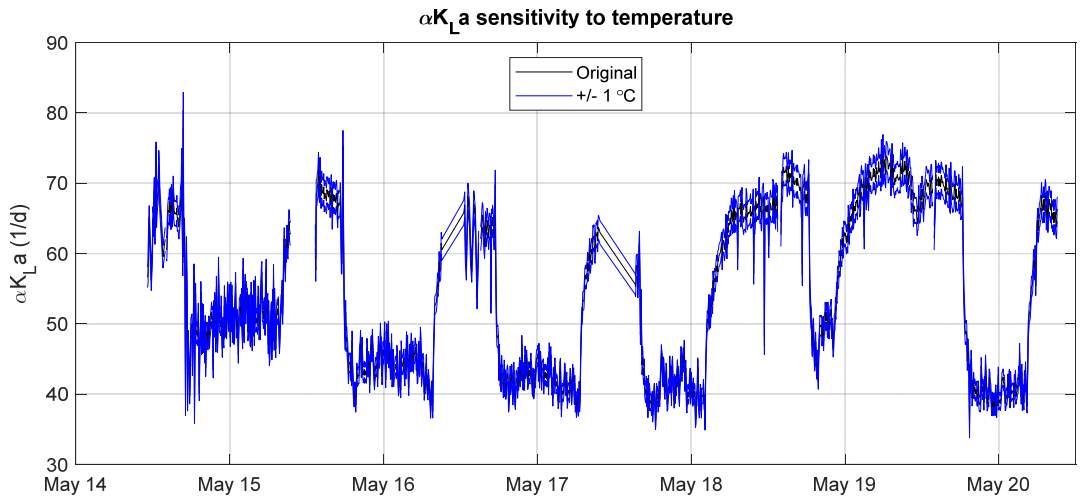
αK_La sensitivity to temperature
Original
+/- 1 °C
αK_La (1/d)
90
80
70
60
50
40
30
May 14
May 15
May 16
May 17
May 18
May 19
May 20

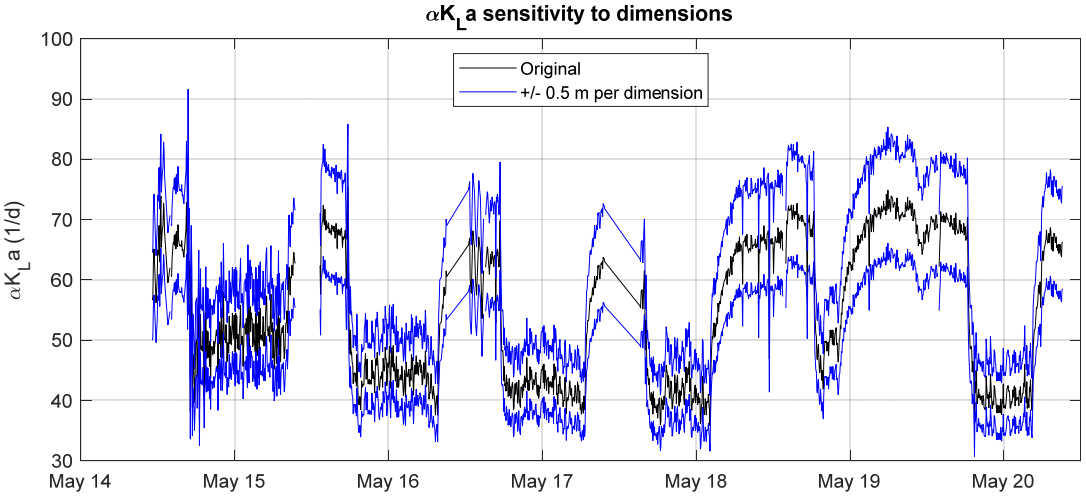
αK_La sensitivity to dimensions
Original
+/- 0.5 m per dimension
αK_La (1/d)
100
90
80
70
60
50
40
30
May 14
May 15
May 16
May 17
May 18
May 19
May 20

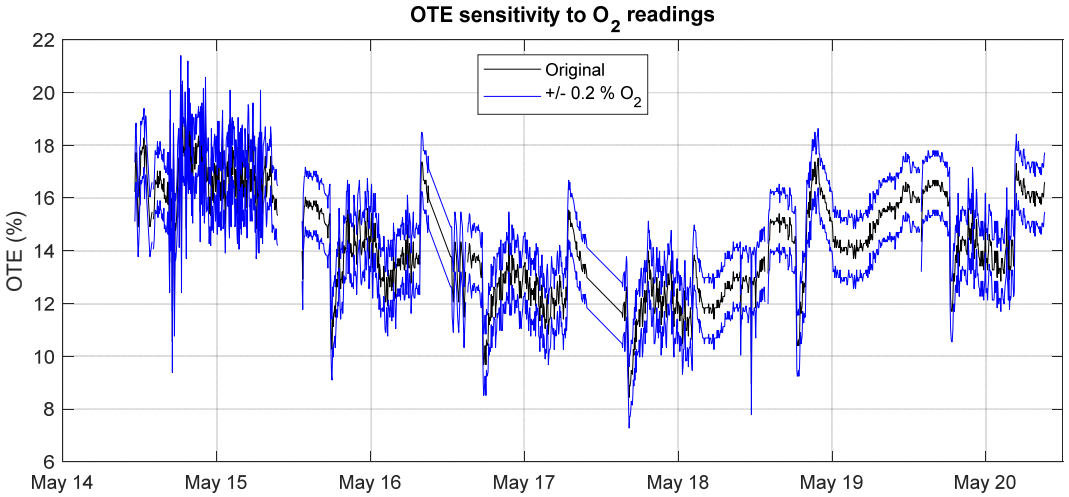
OTE sensitivity to O2 readings
Original
+/- 0.2 % O2
OTE (%)
22
20
18
16
14
12
10
8
6
May 14
May 15
May 16
May 17
May 18
May 19
May 20

A3.2 Manually Recorded Oxygen Transfer Tests

Manual tests are graphed by test number, from 1 to 13, in chronological order. The test details can be seen in Table 3 in section 5.3.

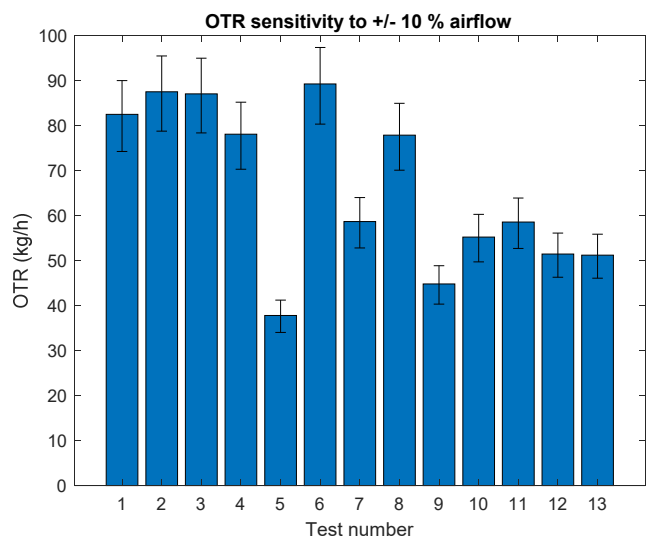

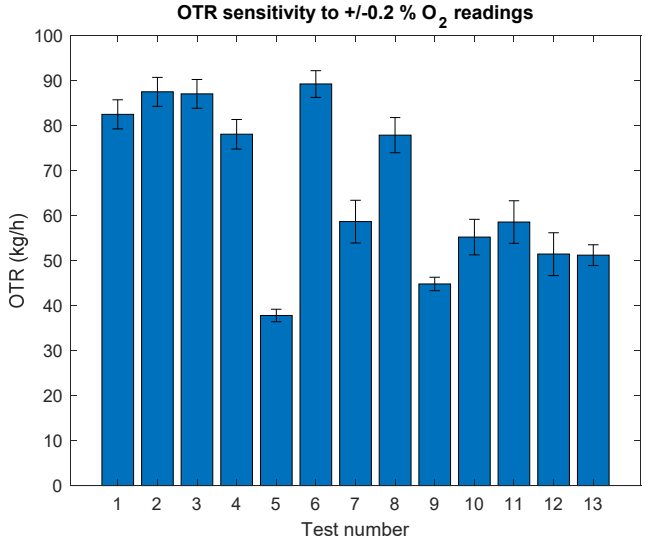

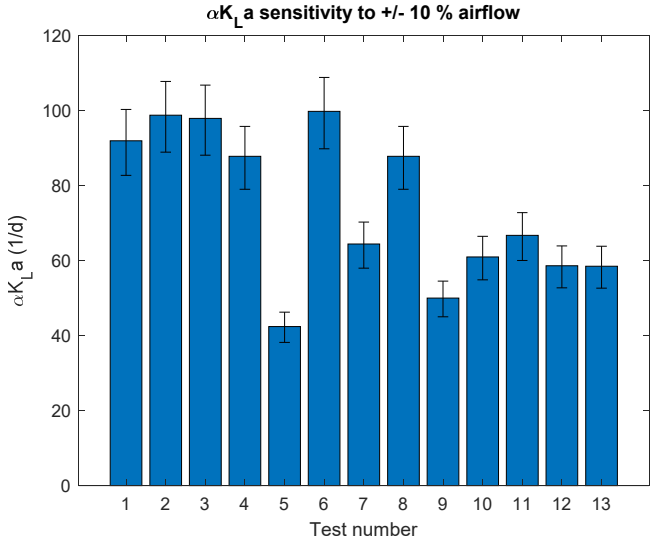

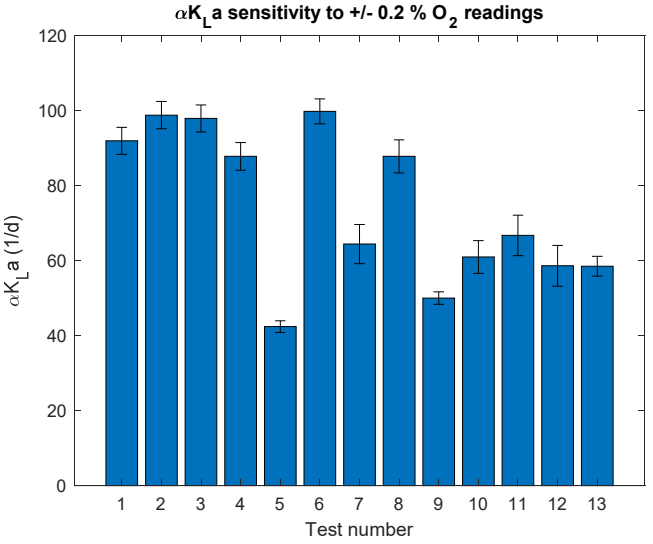

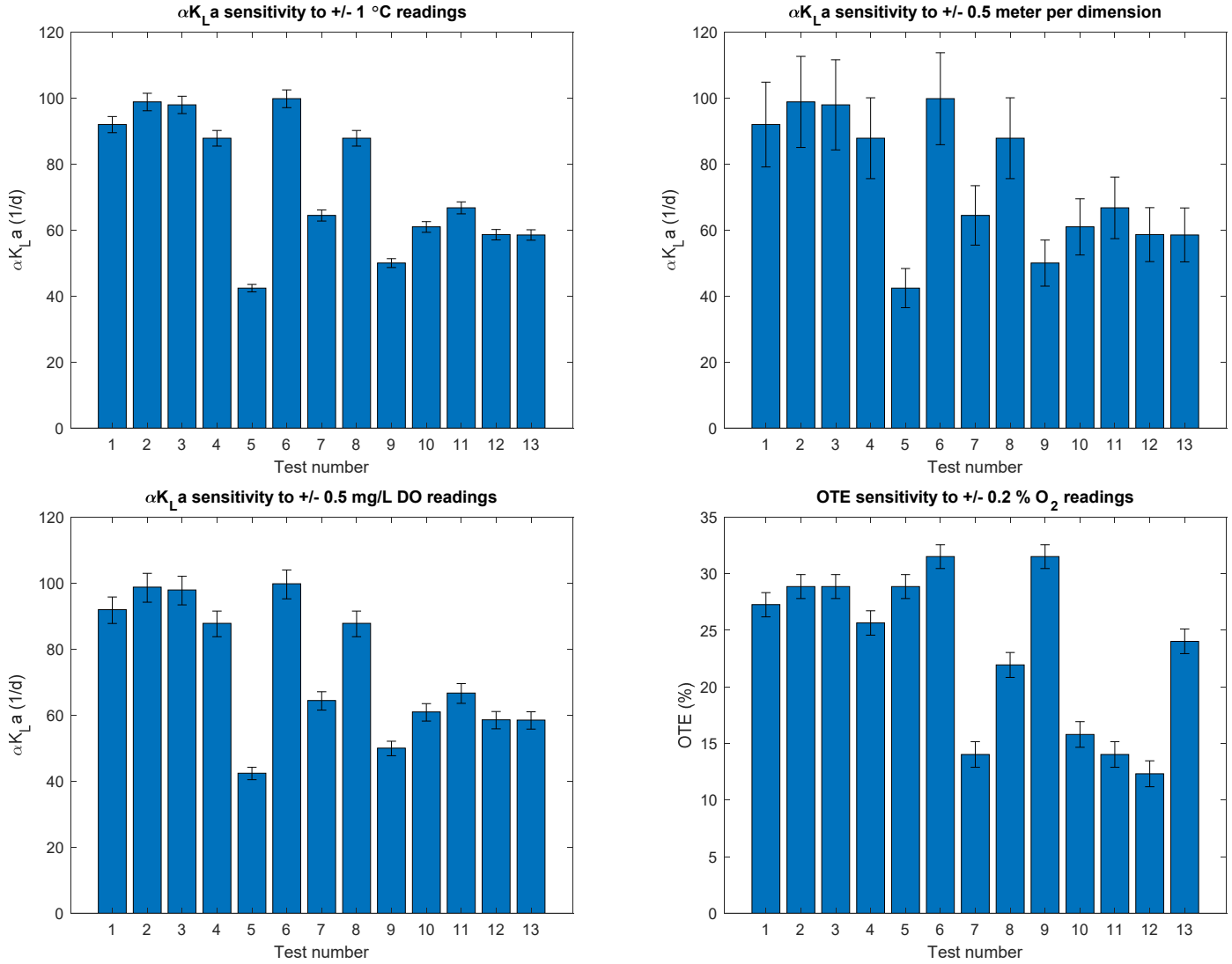

Dimension variations affected related variables the most, followed by air flow variations. It should be noted that for dimension sensitivity a change of 0.5 m was applied to height, width, and depth, resulting in a larger cumulative effect than if only one dimension were altered.

A3.3 Nitrous Oxide Transfer Tests

Continuous N_2O transfer test sensitivity analyses were performed for the effects of variation in measured off-gas N_2O, dissolved N_2O, αK_La, airflow, temperature, and dimensions. The effects of these variations on the most relevant N_2O calculation methods were compared against the measured N_2O and the original calculated N_2O for the same method. Large changes to the selected αK_La value had a significant effect on calculated N_2O, and effects of dimension errors and dissolved N_2O readings were also significant. Temperature seemed to have the least impact on results, and airflow variations had a more significant impact on O_2 method calculations than superficial velocity method calculations, though neither scenario had a large variation.

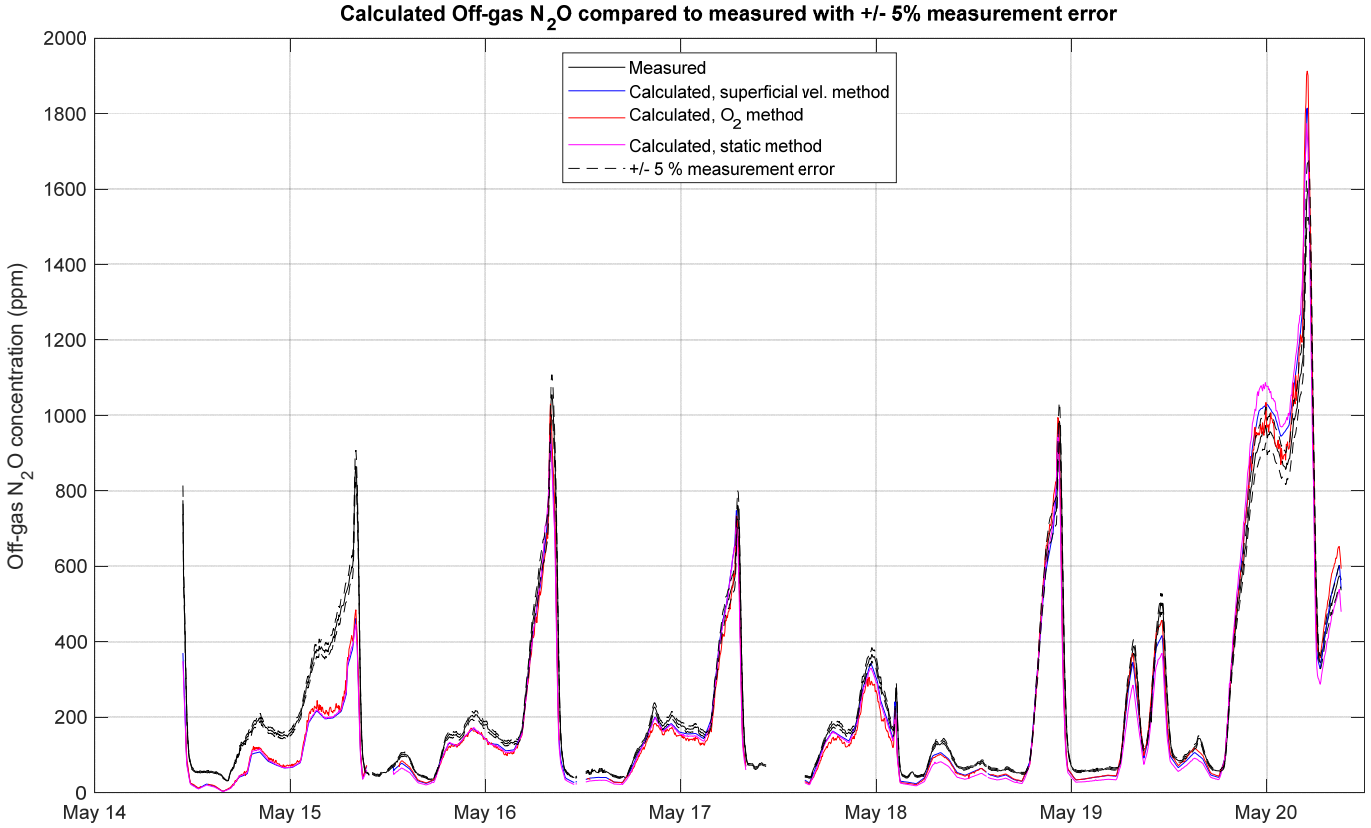

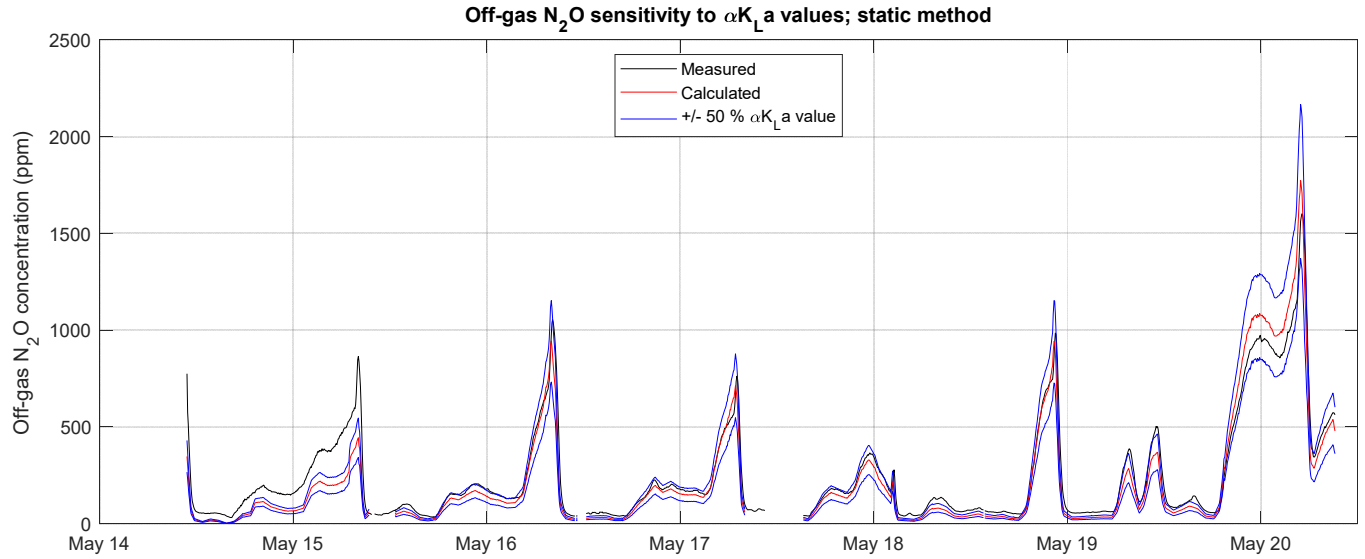
Off-gas N_2O sensitivity to $\alpha K_L a$ values; static method
Off-gas N_2O concentration (ppm)
2500
2000
1500
1000
500
0
Measured
Calculated
+/- 50 % $\alpha K_L a$ value
May 14
May 15
May 16
May 17
May 18
May 19
May 20

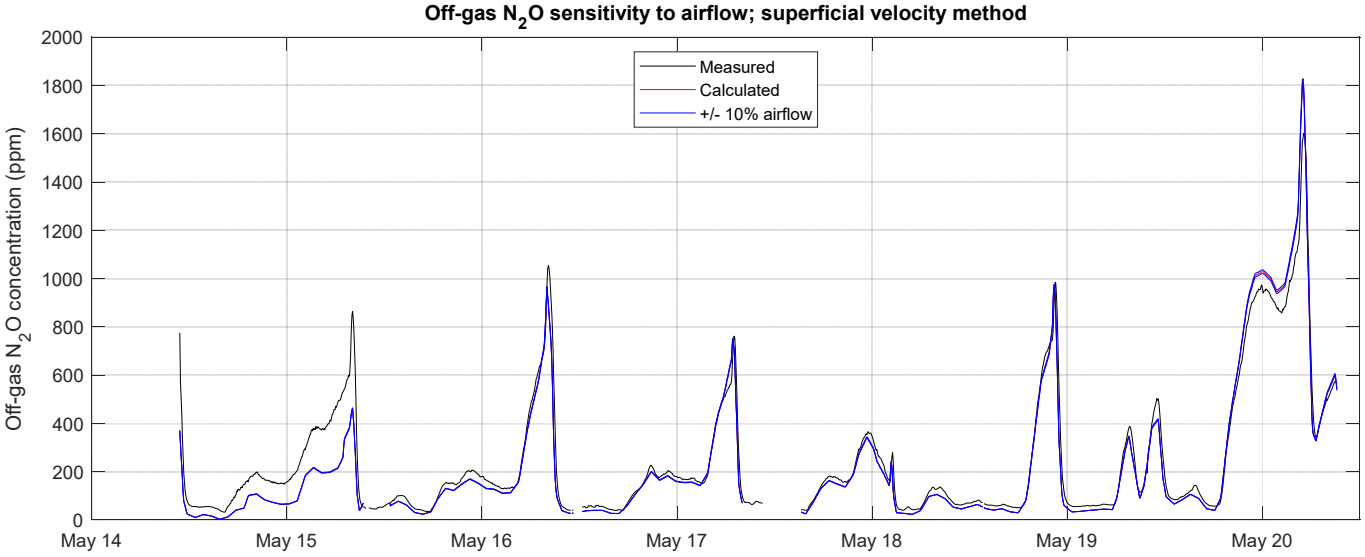
Off-gas N_2O sensitivity to airflow; superficial velocity method
Off-gas N_2O concentration (ppm)
2000
1800
1600
1400
1200
1000
800
600
400
200
0
Measured
Calculated
+/- 10% airflow
May 14
May 15
May 16
May 17
May 18
May 19
May 20

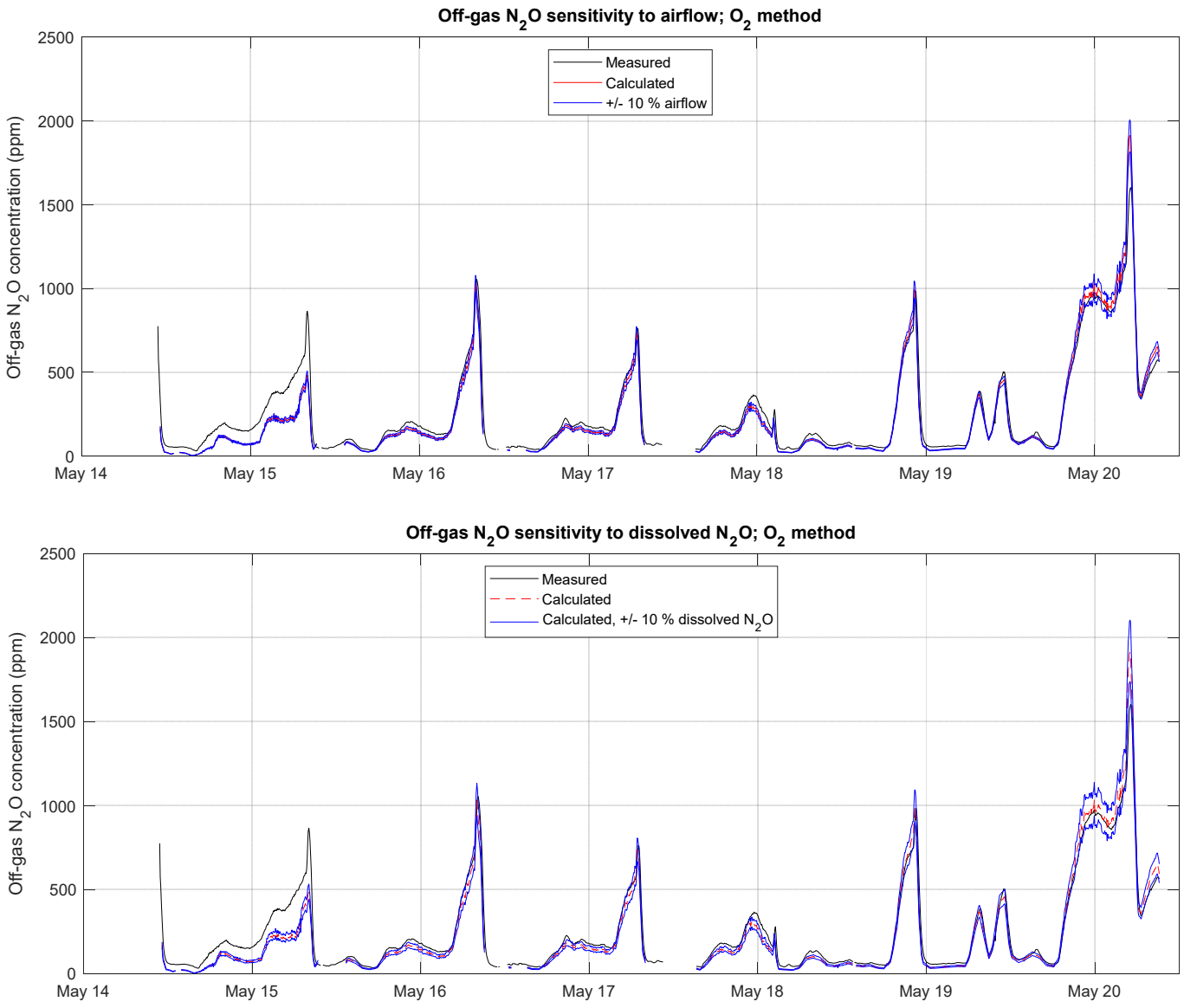
Off-gas N_2O sensitivity to airflow; O_2 method
Measured
Calculated
+/- 10 % airflow
Off-gas N_2O concentration (ppm)
2500
2000
1500
1000
500
0
May 14
May 15
May 16
May 17
May 18
May 19
May 20
Off-gas N_2O sensitivity to dissolved N_2O; O_2 method
Measured
Calculated
Calculated, +/- 10 % dissolved N_2O
Off-gas N_2O concentration (ppm)
2500
2000
1500
1000
500
0
May 14
May 15
May 16
May 17
May 18
May 19
May 20

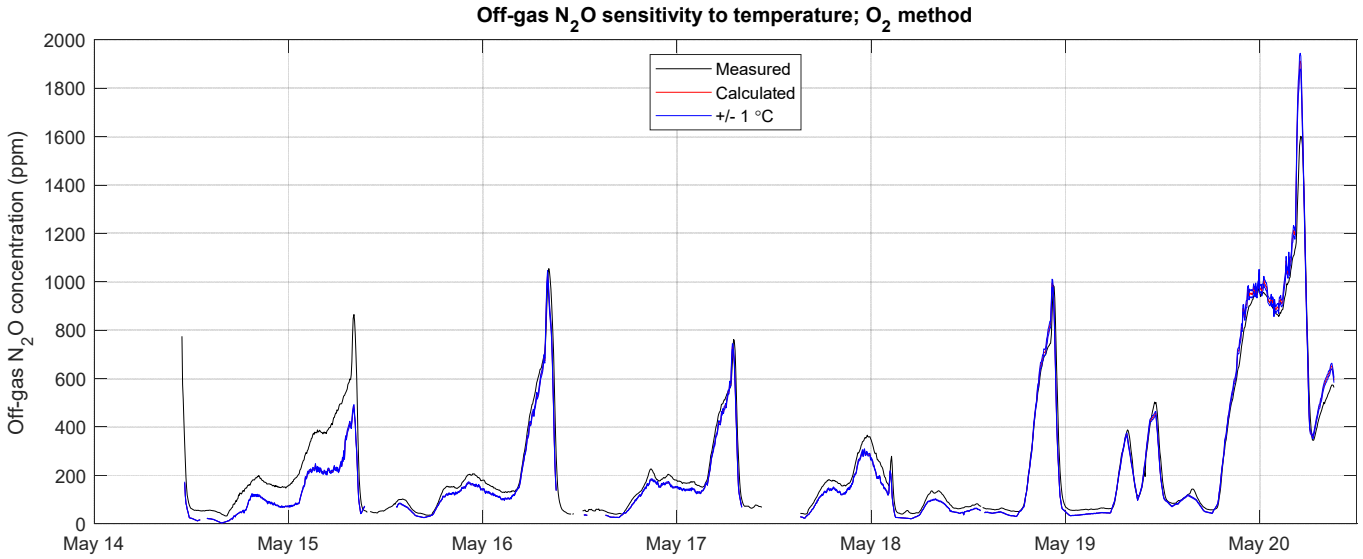
Off-gas N2O sensitivity to temperature; O2 method
Measured
Calculated
+/- 1 °C
Off-gas N2O concentration (ppm)
0
200
400
600
800
1000
1200
1400
1600
1800
2000
May 14
May 15
May 16
May 17
May 18
May 19
May 20

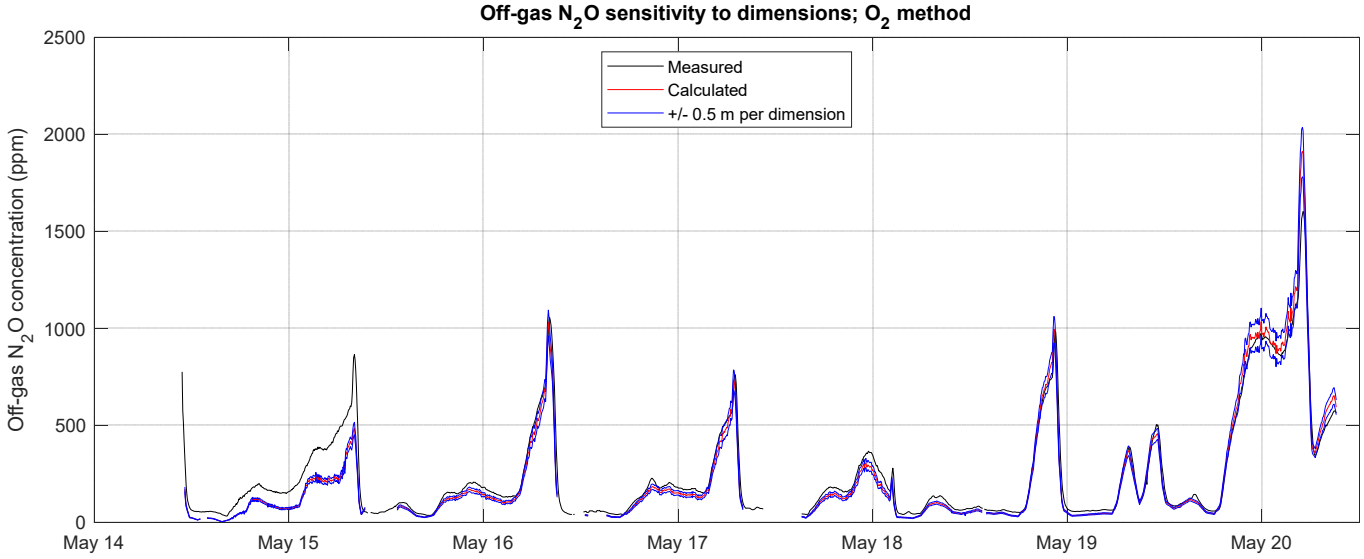
Off-gas N2O sensitivity to dimensions; O2 method
Measured
Calculated
+/- 0.5 m per dimension
Off-gas N2O concentration (ppm)
0
500
1000
1500
2000
2500
May 14
May 15
May 16
May 17
May 18
May 19
May 20